

NBER WORKING PAPER SERIES

OPTION PRICES IN A MODEL WITH STOCHASTIC DISASTER RISK

Sang Byung Seo  
Jessica A. Wachter

Working Paper 19611  
<http://www.nber.org/papers/w19611>

NATIONAL BUREAU OF ECONOMIC RESEARCH  
1050 Massachusetts Avenue  
Cambridge, MA 02138  
November 2013

We thank Hui Chen, Domenico Cuoco, Mikhail Chernov, Xavier Gabaix, Ivan Shaliastovich, Viktor Todorov and seminar participants at the 2013 NBER Summer Institute, Carnegie Mellon University, Cornell University and the Wharton school for helpful comments. The views expressed herein are those of the authors and do not necessarily reflect the views of the National Bureau of Economic Research.

NBER working papers are circulated for discussion and comment purposes. They have not been peer-reviewed or been subject to the review by the NBER Board of Directors that accompanies official NBER publications.

© 2013 by Sang Byung Seo and Jessica A. Wachter. All rights reserved. Short sections of text, not to exceed two paragraphs, may be quoted without explicit permission provided that full credit, including © notice, is given to the source.

Option Prices in a Model with Stochastic Disaster Risk  
Sang Byung Seo and Jessica A. Wachter  
NBER Working Paper No. 19611  
November 2013, Revised August 2015  
JEL No. G12, G13

**ABSTRACT**

Contrary to the Black-Scholes model, volatilities implied by index option prices depend on the exercise price of the option and are often higher than realized volatilities. We explain both facts in the context of a model that can also explain the mean and volatility of equity returns. Our model assumes a small risk of a rare disaster that is calibrated based on the international data on large consumption declines. We allow the risk of this rare disaster to be stochastic, which turns out to be crucial to the model's ability to explain both equity volatility and option prices. We explore different specifications for the stochastic rare disaster probability and show that the data favor a multifrequency process. Finally, we show that the model can simultaneously fit the time series of option prices and equities.

Sang Byung Seo  
Finance Department, The Wharton School  
3620 Locust Walk  
Philadelphia, PA 19104  
sangseo@wharton.upenn.edu

Jessica A. Wachter  
Department of Finance  
2300 SH-DH  
The Wharton School  
University of Pennsylvania  
3620 Locust Walk  
Philadelphia, PA 19104  
and NBER  
jwachter@wharton.upenn.edu

# 1 Introduction

The Black and Scholes (1973) model, which describes option prices in terms of the price and volatility of the underlying asset, is regarded as one of the great achievements in financial economics. Yet since Rubinstein (1994), researchers have noted a striking failure of the model: the volatility implied by the option price varies with the exercise price. The Black-Scholes model says that this implied volatility should be constant and equal to the volatility of the underlying asset.

In the data, the volatility implied by out-of-the-money (OTM) put options – those with an exercise price less than the current stock price – is significantly higher than the volatility implied by at-the-money (ATM) put options – those with an exercise price equal to the current stock price. The fact that the implied volatility tends to decrease as a function “moneyness” (the difference between the stock price and the exercise price divided by the stock price) is known as the volatility skew. The volatility skew implies that OTM put options are expensive relative to ATM put options, because the option price is increasing as a function of implied volatility. Moreover, even ATM implied volatilities are significantly higher than return volatility (Coval and Shumway, 2001), implying that ATM option prices are also expensive relative to the Black-Scholes benchmark.

Why the Black-Scholes model fails is an important and still-unresolved question in the literature. In the Black-Scholes model, the stock price evolves as a log-normal process with constant volatility. Under these assumptions, the stock and riskfree asset complete the market, and so the specification of these two prices suffices to describe the economy. A natural extension is to incorporate stochastic volatility and jumps into stock prices. In these cases, the market cannot be completed by only two assets, and so it is necessary to further specify a pricing kernel to determine how volatility and jump risk are priced. In one line of work, this pricing kernel (along with the stock price and riskfree rate) is specified exogenously.

This “reduced form” approach has been successful in explaining average implied volatilities (see, for example, Bates (2000), Broadie, Chernov, and Johannes (2007), Eraker (2004), Pan (2002), Santa-Clara and Yan (2010)).<sup>1</sup> Ultimately, however, both the pricing kernel and the stock price are endogenous objects. A deeper explanation of option prices thus requires the same approach as in other types of asset pricing: a utility function together with a process for the endowment and cash flows.

The purpose of this paper is to build such a model to explain implied volatilities. The reduced-form literature suggests that non-normalities are important, and so a natural approach is to consider a model with disaster risk, as in Barro (2006) and Rietz (1988). Backus, Chernov, and Martin (2011) show that while this disaster-risk model indeed implies a volatility skew, the size of the skew is far greater than in the data. One interpretation of their findings is that information from option prices and from macroeconomic events are inconsistent; perhaps the international data are simply not relevant for U.S. investors, who indeed are allowing for jumps, but of a far smaller magnitude. Because rare disaster models do rely on the international data to explain the equity premium, this appears to be a dramatic rejection of this model.

We show, however, that a more general rare disasters model can explain implied volatilities. In fact, the very same generalization that allows the models of Barro (2006) and Rietz (1988) to explain stock market volatility also enables the model to explain options data. This generalization is to allow the probability of a disaster to be stochastic in a setting with a preference for early resolution of uncertainty. Under these conditions, rare disasters can explain both the equity premium and stock market volatility.<sup>2</sup> Moreover, the model implies that that volatility is priced, so that implied volatilities are higher than realized volatilities,

---

<sup>1</sup>In earlier work, Stutzer (1996) also finds a role for non-normal distributions in explaining implied volatilities.

<sup>2</sup>See Gabaix (2012), Gourio (2012) and Wachter (2013) for rare disaster models that explain stock price volatility. This paper builds off of Wachter (2013).

as in the data.

Besides explaining implied volatilities across a range of exercise prices and times to expiration, we also ask the model to explain the volatilities of volatilities, and, what turns out to be harder, the volatility of the slope in the implied volatility curve. While at the money implied volatilities say something about current volatility in stock prices, out-of-the money volatilities say more about tail risk. In the data, these do not move one-for-one; however in the simplest version of the model, they do. We show how introducing richer dynamics for the probability of a disaster allows the model to account for the time-variation in this slope that is present in the data. Given this model's success in matching option prices along various dimensions, we can back out the state variables using the time series of option prices. The equity prices implied by this time series line up well with the equity prices in the data.

Our model builds on a previous literature on option pricing in endowment economies. Gabaix (2012) develops a framework with stochastic rare-event sensitivity to match a variety of asset pricing facts, one of which is the volatility skew. For tractability reasons, he uses a different model to price options than that used to price equities. Our model differs in that we assume time-variation in the probability of a disaster; as we show, this mechanism can explain both realized stock market volatility as well as option-implied volatility. It is tractable enough so that it can simultaneously price options and equities, and it nests the iid case previously emphasized in the literature (e.g. Backus, Chernov, and Martin (2011)), which makes the difference in the results transparent. We also consider a wider range of option pricing facts, including patterns in the implied volatility surface (namely how implied volatilities vary with maturity as well as exercise price) and time-variation in the slope of the volatility skew.<sup>3</sup> Other models explain the volatility skew, but unlike ours, use non-standard beliefs or preferences. We discuss these in Section 3.4

---

<sup>3</sup>Recent work by Nowotny (2011) reports average implied volatilities as well. Nowotny focuses on the implications of self-exciting processes for equity markets rather than on option prices.

A growing line of empirical work uses option prices to estimate time-varying risks of rare events and their impact on risk premia. Bollerslev and Todorov (2011) show that a substantial fraction of the equity premium can be attributable to jump risk reflected in option prices, Gao and Song (2013) price crash risk in the cross-section using options, and Kelly, Pastor, and Veronesi (2014) demonstrate a link between options and political risk. The results in these papers provide empirical support for the theoretical mechanism that we highlight, namely that options reflect the risk of economy-wide rare events, and that this risk varies over time.

The remainder of this paper is organized as follows. Section 2 introduces a multifrequency stochastic disaster risk (SDR) model, and discusses the solution for equity prices and options. A limiting case of this model has a single state variable following a Cox, Ingersoll, and Ross (1985) process. As we show in Section 3, this limiting case can explain the level and slope of the implied volatility skew, as well as the mean and volatility of stock prices. This section explains why allowing the disaster probability to be stochastic makes a qualitative difference in the model's ability to explain implied volatilities. However, this single-frequency model is not sufficient to explain the *variation* in the skew over time. For this, the more general model is needed, as we show in Section 4. This section also shows that the time series of state variables implied by option prices are also capable of explaining the time series of aggregate market prices. Section 5 concludes.

## **2 A multifrequency model with stochastic disaster risk**

This section describes our multifrequency model for stochastic disaster risk. For convenience, we describe the most general model we need in detail. However, a more restrictive model is all that is necessary for many of our results, as we explain. Section 2.1 describes the model assumptions, Section 2.2 describes the solution for equity prices. Given these equity

prices, Section 2.3 describes how we solve for options on equities. Section 2.4 describes how a single-frequency model is a limiting case of the multifrequency model, and how a constant disaster risk model is a limiting case of the single-frequency model.

## 2.1 Assumptions

We assume a complete-markets endowment economy with an infinitely-lived representative agent. Aggregate consumption (the endowment) solves the following stochastic differential equation

$$dC_t = \mu C_{t-} dt + \sigma C_{t-} dB_t + (e^{Z_t} - 1)C_{t-} dN_t, \quad (1)$$

where  $B_t$  is a standard Brownian motion and  $N_t$  is a Poisson process with time-varying intensity  $\lambda_t$ . For the range of parameter values we consider,  $\lambda_t$  is small and can therefore be interpreted to be (approximately) the probability of a jump. We thus use the terminology probability and intensity interchangeably, while keeping in mind that the relation is an approximate one. We allow the jump intensity to follow a multifrequency process:

$$d\lambda_t = \kappa_\lambda(\xi_t - \lambda_t)dt + \sigma_\lambda \sqrt{\lambda_t} dB_{\lambda,t}, \quad (2)$$

where

$$d\xi_t = \kappa_\xi(\bar{\xi} - \xi_t)dt + \sigma_\xi \sqrt{\xi_t} dB_{\xi,t}, \quad (3)$$

and where all Brownian motions are independent.<sup>4</sup>

The size of a jump, provided that a jump occurs, is determined by  $Z_t$ . We assume  $Z_t$  is a random variable whose time-invariant distribution  $\nu$  is independent of  $N_t$ ,  $B_t$  and  $B_{\lambda,t}$ .

---

<sup>4</sup>Multifrequency processes for volatility have been shown to be important for matching option prices in the context of reduced-form models (Andersen, Fusari, and Todorov (2013), Bates (2000), Christoffersen, Heston, and Jacobs (2009), and Gallant, Hsu, and Tauchen (1999)). Our model differs from these in that we specify a process for the disaster risk, and because volatility is endogenous in our model, rather than exogenous.

We use the notation  $E_\nu$  to denote expectations of functions of  $Z_t$  taken with respect to the  $\nu$ -distribution. The  $t$  subscript on  $Z_t$  will be omitted when not essential for clarity.

We assume a recursive generalization of power utility that allows for preferences over the timing of the resolution of uncertainty. Our formulation comes from Duffie and Epstein (1992), and we consider a special case in which the elasticity of intertemporal substitution (EIS) is equal to 1. That is, we define continuation utility  $V_t$  for the representative agent using the following recursion:

$$V_t = E_t \int_t^\infty f(C_s, V_s) ds, \quad (4)$$

where

$$f(C, V) = \beta(1 - \gamma)V \left( \log C - \frac{1}{1 - \gamma} \log((1 - \gamma)V) \right). \quad (5)$$

The parameter  $\beta$  is the rate of time preference and  $\gamma$  is the coefficient of relative risk aversion. This utility function is equivalent to the continuous-time limit (and the limit as the EIS approaches one) of the utility function defined by Epstein and Zin (1989) and Weil (1990).

## 2.2 Solving for asset prices

We solve for asset prices using the state-price density,  $\pi_t$ . Duffie and Skiadas (1994) characterize the state-price density as

$$\pi_t = \exp \left\{ \int_0^t \frac{\partial}{\partial V} f(C_s, V_s) ds \right\} \frac{\partial}{\partial C} f(C_t, V_t). \quad (6)$$

There is an equilibrium relation between utility  $V_t$ , consumption  $C_t$  and the disaster probability  $\lambda_t$ . Namely,

$$V_t = \frac{C_t^{1-\gamma}}{1-\gamma} e^{a+b\lambda\lambda_t+b\xi\xi_t}$$

where

$$a = \frac{1-\gamma}{\beta} \left( \mu - \frac{1}{2}\gamma\sigma^2 \right) + \frac{b_\xi \kappa_\xi \bar{\xi}}{\beta} \quad (7)$$

$$b_\lambda = \frac{\kappa_\lambda + \beta}{\sigma_\lambda^2} - \sqrt{\left( \frac{\kappa_\lambda + \beta}{\sigma_\lambda^2} \right)^2 - 2 \frac{E_\nu [e^{(1-\gamma)Z_t} - 1]}{\sigma_\lambda^2}} \quad (8)$$

$$b_\xi = \frac{\kappa_\xi + \beta}{\sigma_\xi^2} - \sqrt{\left( \frac{\kappa_\xi + \beta}{\sigma_\xi^2} \right)^2 - 2 \frac{b_\lambda \kappa_\lambda}{\sigma_\xi^2}} \quad (9)$$

It follows that the state-price density can be written as

$$\pi_t = \exp \left( -\beta(a+1)t - \beta b_\lambda \int_0^t \lambda_s ds - \beta b_\xi \int_0^t \xi_s ds \right) \beta C_t^{-\gamma} e^{a+b_\lambda \lambda_t + b_\xi \xi_t}. \quad (10)$$

Details are provided in Appendix B.2.

We assume a standard model for dividends (Campbell (2003), Abel (1999)):  $D_t = C_t^\phi$ , for leverage parameter  $\phi$ .<sup>5</sup> Let  $F(D_t, \lambda_t, \xi_t)$  be the value of the aggregate market (it will be apparent in what follows that  $F$  is a function of  $D_t$ ,  $\lambda_t$  and  $\xi_t$ ). It follows from no-arbitrage that

$$F(D_t, \lambda_t, \xi_t) = E_t \left[ \int_t^\infty \frac{\pi_s}{\pi_t} D_s ds \right].$$

The stock price can be written explicitly as

$$F(D_t, \lambda_t, \xi_t) = D_t G(\lambda_t, \xi_t), \quad (11)$$

---

<sup>5</sup>This implies that dividends respond more than consumption to disasters, an assumption that is plausible given the U.S. data (Longstaff and Piazzesi (2004)). As elsewhere in the literature on endowment economies, we take the disconnect between consumption and dividends as given. The assumption of leverage is not crucial in that we would obtain similar results in a model with no leverage and a higher value of the EIS.

where the price-dividend ratio  $G$  is given by

$$G(\lambda_t, \xi_t) = \int_0^\infty \exp(a_\phi(\tau) + b_{\phi\lambda}(\tau)\lambda_t + b_{\phi\xi}(\tau)\xi_t) d\tau, \quad (12)$$

where  $a_\phi$ ,  $b_{\phi\lambda}$  and  $b_{\phi\xi}$  solve the differential equations

$$\begin{aligned} a'_\phi(\tau) &= -\beta + (\phi - 1)\mu + \left(\frac{1}{2}\phi - \gamma\right)(\phi - 1)\sigma^2 + b_{\phi\xi}(\tau)\kappa_\xi\bar{\xi} \\ b'_{\phi\lambda}(\tau) &= -b_{\phi\lambda}(\tau)\kappa_\lambda + \frac{1}{2}b_{\phi\lambda}(\tau)^2\sigma_\lambda^2 + b_\lambda b_{\phi\lambda}(\tau)\sigma_\lambda^2 + E_\nu[e^{(\phi-\gamma)Z_t} - e^{(1-\gamma)Z_t}] \\ b'_{\phi\xi}(\tau) &= -b_{\phi\lambda}(\tau)\kappa_\lambda - b_{\phi\xi}(\tau)\kappa_\xi + \frac{1}{2}b_{\phi\xi}(\tau)^2\sigma_\xi^2 + b_\xi b_{\phi\xi}(\tau)\sigma_\xi^2, \end{aligned}$$

with boundary condition

$$a_\phi(0) = b_{\phi\lambda}(0) = b_{\phi\xi}(0) = 0.$$

(see Appendix B.3). We will often use the abbreviation  $F_t = F(D_t, \lambda_t, \xi_t)$  to denote the value of the stock market index at time  $t$ .

### 2.3 Solving for implied volatilities

Let  $P(F_t, \lambda_t, \xi_t, \tau; K)$  denote the time- $t$  price of a European put option on the stock market index with strike price  $K$  and expiration  $t + \tau$ . For simplicity, we will abbreviate the formula for the price of the dividend claim as  $F_t = F(D_t, \lambda_t, \xi_t)$ . Because the payoff on this option at expiration is  $(K - F_{t+\tau})^+$ , it follows from the absence of arbitrage that

$$P(F_t, \lambda_t, \xi_t, T - t; K) = E_t \left[ \frac{\pi_T}{\pi_t} (K - F_T)^+ \right].$$

Let  $K^n = K/F_t$ , the normalized strike price (or “moneyness”), and define

$$P^n(\lambda_t, \xi_t, T - t; K^n) = E_t \left[ \frac{\pi_T}{\pi_t} \left( K^n - \frac{F_T}{F_t} \right)^+ \right]. \quad (13)$$

We will establish below that  $P^n$  is indeed a function of  $\lambda_t$ , time to expiration and moneyness alone. Clearly  $P_t^n = P_t/F_t$ . Because our ultimate interest is in implied volatilities, and because, in the formula of Black and Scholes (1973), normalized option prices are functions of the normalized strike price (and the volatility, interest rate and time to maturity), it suffices to calculate  $P_t^n$ .<sup>6</sup>

Returning to the formula for  $P_t^n$ , we note that, from (11), it follows that

$$\frac{F_T}{F_t} = \frac{D_T}{D_t} \frac{G(\lambda_T, \xi_T)}{G(\lambda_t, \xi_t)}. \quad (14)$$

Moreover, it follows from (10) that

$$\frac{\pi_T}{\pi_t} = \left( \frac{C_T}{C_t} \right)^{-\gamma} \exp \left\{ \int_t^T -\beta(1 + a + b_\lambda \lambda_s + b_\xi \xi_s) ds + b_\lambda(\lambda_T - \lambda_t) + b_\xi(\xi_T - \xi_t) \right\}. \quad (15)$$

At time  $t$ ,  $\lambda_t$  and  $\xi_t$  are sufficient to determine the distributions of consumption and dividend

---

<sup>6</sup>Given stock price  $F$ , strike price  $K$ , time to maturity  $T - t$ , interest rate  $r$ , and dividend yield  $y$ , the Black-Scholes put price is defined as

$$\text{BSP}(F, K, T - t, r, y, \sigma) = e^{-r(T-t)} KN(-d_2) - e^{-y(T-t)} FN(-d_1)$$

where

$$d_1 = \frac{\log(F/K) + (r - y + \sigma^2/2)(T - t)}{\sigma\sqrt{T - t}} \quad \text{and} \quad d_2 = d_1 - \sigma\sqrt{T - t}$$

Given the put prices calculated from the transform analysis, inversion of this Black-Scholes formula gives us implied volatilities. Specifically, the implied volatility  $\sigma_t^{\text{imp}} = \sigma^{\text{imp}}(\lambda_t, T - t; K^n)$  solves

$$P_t^n(\lambda_t, T - t; K^n) = \text{BSP} \left( 1, K^n, T - t, r_t^b, 1/G(\lambda_t), \sigma_t^{\text{imp}} \right)$$

where  $r_t^b$  is the model’s analogue of the Treasury Bill rate, which allows for a probability of a default in case of a disaster (see Barro (2006); as in that paper we assume a default rate of 0.4).

growth between  $t$  and  $T$ , as well as the distributions of future values of  $\lambda_s$  and  $\xi_s$ ,  $s = 1, \dots, T$ . It follows that normalized put prices (and therefore implied volatilities) are a function of  $\lambda_t$ ,  $\xi_t$ , the time to expiration, and moneyness.

To calculate normalized put prices, we use the transform analysis of Duffie, Pan, and Singleton (2000), applied to a highly-accurate log-linear approximation of the price-dividend ratio. This analytical method avoids the curse of dimensionality and the need to simulate the expectation in (13) which is inefficient due to rare events. See Appendix D for details.

## 2.4 Limiting cases

Setting the high-frequency state variable  $\xi_t$  to a constant results in the single-frequency SDR model considered by Wachter (2013). For ease of notation, we will let  $\bar{\lambda} = \bar{\xi}$  be the mean of  $\lambda_t$  when discussing this single-frequency model. In what follows, we will refer to this as the single-frequency SDR model, or simply, the SDR model, while the general case will always be called the multifrequency model.

Further setting  $\lambda_t$  to a constant  $\bar{\lambda}$  results in a model with constant disaster risk. In this iid model, the EIS and the discount rate are not separately identified and so the model with recursive utility is isomorphic to one with power utility. Thus this model is equivalent to that considered by Barro (2006), Rietz (1988) and Backus, Chernov, and Martin (2011). We refer to this model as the constant disaster risk (CDR) model. Appendix C.2 shows that this limit is indeed well-defined and is what would be computed if one were to solve the constant disaster risk model from first principles. Note that, for the CDR model, the assumption of recursive utility is observationally equivalent to that of power utility (see Tallarini (2000); we establish this fact for our setting in Appendix C.3).

### 3 Average implied volatilities in a single-frequency model

We first consider average implied volatilities, as these are the focus of the prior literature (see, for example, Backus, Chernov, and Martin (2011) and Drechsler (2013)). To highlight the main mechanism of the model, we consider the (single-frequency) SDR model described in Section 2.4 (see Appendix C.1 for more details). To ensure the model also matches equity data, we use the same parameters as Wachter (2013). Thus parameters are chosen for this model without appeal to option prices.

We will compare our results to the findings of Backus, Chernov, and Martin (2011), and thus use their parameters for the CDR model.<sup>7</sup> The two calibrations differ in their relative risk aversion, in the volatility of normal-times consumption growth, in leverage, in the probability of a disaster, and of course in whether the probability is time-varying. The net effect of some of these differences turns out to be less important than what one may think: for example, higher risk aversion and lower disaster probability roughly offset each other.<sup>8</sup> We explore the implications of leverage and volatility in what follows.

The two models also assume different disaster distributions. For the SDR model, the disaster distribution is multinomial, and taken from Barro and Ursúa (2008) based on actual consumption declines. The benchmark CDR model assumes that consumption declines are log-normal. For comparison, we plot the smoothed density for the SDR model along with the density of the consumption-based model in Figure 1. Compared with the lognormal model, the SDR model has more mass over small declines in the 10–20% region, and more mass over large declines in the 50–70% region.<sup>9</sup>

---

<sup>7</sup>In the terminology of Backus et al., this is the “consumption-based model”. We consider a calibration that is isomorphic to their power utility case in the sense described in Section 2.4, and use their assumption of a riskfree rate of 2% to back out a discount rate.

<sup>8</sup>In fact, the results are very similar if we use the same parameters as in the SDR model, except with  $\sigma_\lambda = 0$ .

<sup>9</sup>One concern is the sensitivity of our results to behavior in the tails of the distribution. By assuming a multinomial distribution, we essentially assume that this distribution is bounded, which is probably not

The volatility skew in the data represents an average of implied volatilities at different points in time. We follow the same procedure in the model, calculating an unconditional average volatility skew. To do so, we first solve for the implied volatility as a function of  $\lambda_t$ . We numerically integrate this function over the stationary distribution of  $\lambda_t$ . This stationary distribution is Gamma with shape parameter  $2\kappa\bar{\lambda}/\sigma_\lambda^2$  and scale parameter  $\sigma_\lambda^2/(2\kappa)$  (Cox, Ingersoll, and Ross (1985)).

Figure 2 shows the resulting implied volatilities as a function of moneyness, as well as implied volatilities in the data. Confirming previous results, we find that the CDR model leads to implied volatilities that are dramatically different from those in the data. First, the implied volatilities are too low, even though the model was calibrated to match the volatility of equity returns. Second, they exhibit a strong downward slope as a function of the strike price. While there is a downward slope in the data, it is not nearly as large. As a result, implied volatilities for ATM options in the CDR model are less than 10%, far below the option-based implied volatilities, which are over 20%.

In contrast, the SDR model can explain both ATM and OTM implied volatilities. For OTM options with moneyness equal to 0.94, the SDR model gives an implied volatility of 23%, close to the data value of 24%. There is a downward slope, just as in the data, but it is much smaller than that of the CDR model. ATM options have implied volatilities of about 21% in both the model and the data. There are a number of differences between this model and the CDR model. We now discuss which of these differences is primarily responsible for the change in implied volatilities.

---

realistic. However, it makes very little difference if we consider a unbounded distribution that matches the observations in the data. Barro and Jin (2011) suggest this can be done with a power law distribution with tail parameter of about 6.5. We have tried this version of the model and the results are virtually indistinguishable. The reason is that, even though low realizations are possible in theory, their probability is so small as to not affect the model's results.

### 3.1 The role of leverage

In their discussion, Backus, Chernov, and Martin (2011) emphasize the role of very bad consumption realizations as a reason for the poor performance of the disaster model. Therefore, this seems like an appropriate place to start. The disaster distribution in the SDR benchmark actually implies a slightly higher probability of extreme events than the benchmark CDR model (Figure 1). However, the benchmark CDR model has much higher leverage: the leverage parameter is 5.1 for the CDR calibration versus 2.6 for the SDR calibration. Leverage does not affect consumption but it affects dividends, and therefore stock and option prices. A higher leverage parameter implies that dividends will fall further in the event of a consumption disaster. It is reasonable, therefore, to attribute the difference in the implied volatilities to the difference in the leverage parameter.

Figure 3 tests this directly by showing option prices in the CDR model for leverage of 5.1 and for leverage of 2.6 (denoted “lower leverage”) in the figure. Surprisingly, the slope for the calibration with leverage of 2.6 is slightly higher than the slope for leverage of 5.1. Lowering leverage results in a downward shift in the level of the volatility skew, not the slope. Thus the difference in leverage cannot be the explanation for why the slope in our model is lower than the slope for CDR.

Why does the change in leverage result in a shift in the level of the skew? It turns out that in the CDR model, changing normal-times volatility has a large effect. Leverage affects both the disaster distribution and normal-times volatility. Lowering leverage has a large effect on normal-times volatility and thus at-the-money options. This is why the level of the curve is lower, and the slope is slightly steeper.<sup>10</sup>

---

<sup>10</sup>Yan (2011) shows analytically that, as the time to expiration approaches zero, the implied volatility is equal to the normal-times volatility in the stock price, while the slope is inversely related to the normal-times volatility of the stock price.

### 3.2 The role of normal shocks in consumption

To further consider the role of normal-times volatility, we explore the impact of changing the consumption volatility parameter  $\sigma$ . In the benchmark CDR comparison, consumption volatility is equal to the value of consumption volatility over the 1889–2009 sample, namely 3.5%. Most of this volatility is accounted for by the disaster distribution, because, while the disasters are rare, they are severe. Therefore normal-times volatility is 1%, lower than the U.S. consumption volatility over the post-war period. The SDR model is calibrated differently; following Barro (2006), the disaster distribution is determined based on international macroeconomic data, and the normal-times distribution is set to match postwar volatility in developed countries. The resulting normal-times volatility is 2%. To evaluate the effect of this difference, we solve for implied volatilities in the CDR model with leverage of 5.1 and normal-times volatility of 2%. In Figure 3, the result is shown in the line denoted “higher normal-times volatility.”

As Figure 3 shows, increasing the normal-times volatility of consumption growth in the CDR model has a noticeable effect on implied volatilities: The implied volatility curve is higher and flatter. The change in the level reflects the greater overall volatility. The change in the slope reflects the greater probability of small, negative outcomes. However, the effect, while substantial, is not nearly large enough to explain the full difference. The level of the “higher normal-times volatility” smile is still too low and the slope is too high compared with the data.<sup>11</sup>

While raising the volatility of consumption makes the CDR model look somewhat more like the SDR model, it is not the case that lowering the volatility of consumption makes the SDR model more like the CDR model. Namely, reducing  $\sigma$  to 1% (which would imply

---

<sup>11</sup>Note further that leverage of 5.1, combined with a normal-times consumption volatility of 2% means that normal-times dividend volatility of dividends is 10.2%. However, annual volatility in postwar data is only 6.5%.

a normal-times consumption volatility that is lower than in the post-war data) has almost no effect on the implied volatility curve of the SDR model. There are two reasons why this parameter affects implied volatilities differently in the two cases. First, the leverage parameter is much lower in the SDR model than the CDR model. Second, volatility in the SDR model comes from time-variation in discount rates (driven by  $\lambda_t$ ) as well as in payouts ( $\phi\sigma$ ). The first of these terms is much larger than the second.<sup>12</sup>

### 3.3 The role of stock price volatility in normal times

We showed above that, while normal-times volatility in consumption determines the skew in the CDR model, it does not for the SDR model because, in the SDR model, consumption volatility has a negligible impact on stock prices. What drives stock prices is time-variation in the disaster probability  $\lambda_t$ . When  $\lambda_t$  rises, risk premia on stocks rise, causing fluctuations in asset prices beyond what one would see from the realization of disasters themselves.

This normal-times fluctuation in stock prices is crucial for matching the level and slope of the volatility skew. Normal-times volatility in stock prices generates high implied volatilities for ATM options. Moreover, because of the importance of normal shocks ( $\lambda_t$  follows a diffusion), the slope is shallow for ATM options.<sup>13</sup> In contrast, while the CDR model can match the unconditional volatility in the market, the entirety of this volatility occurs during periods with disasters. Thus ATM implied volatilities are low, and, because of the importance of jump risk, the skew is very steep.

---

<sup>12</sup>To be precise, total return volatility in the SDR model equals the square root of the variance due to  $\lambda_t$ , plus the variance in dividends. Dividend variance is small, and it is added to something much larger to determine total variance. Thus the effect of dividend volatility on return volatility is very small, and changes in dividend volatility also have relatively little effect.

<sup>13</sup>In a reduced-form model, Yan (2011) shows analytically that, as the time to expiration approaches zero, the implied volatility for ATM options is equal to the normal-times volatility in the stock price, while the slope is inversely related to the normal-times volatility of the stock price.

Note that the success in matching implied volatilities comes about simply by making a constant parameter stochastic. Even though average implied volatilities are an *unconditional* moment of the data, a change in the *conditional* distribution in the model has a large effect. The results are in stark contrast to the impact of a similar exercise in a reduced-form model.<sup>14</sup> The reason is that, in an equilibrium model like the present one, unconditional stock market volatility arises endogenously from conditional moments of fundamentals. While it is possible to match the unconditional volatility of stock returns and consumption in an iid model, this can only be done by having all of the volatility occur during disasters. In such a model it is not possible to generate sufficient stock market volatility in normal times to match either implied or realized volatilities. While in the reduced-form literature, the difference between iid and dynamic models principally affects the conditional second moments, in the equilibrium literature, the difference affects the level of volatility itself.

The SDR model contains an additional mechanism that further increases ATM volatilities above the level of realized volatility. This mechanism is embedded in recursive utility. Recursive utility plays a number of roles in the model, including enabling the model to match realized volatilities; without recursive utility, the price-dividend ratio would not fall on an increased risk of rare disasters, because, at reasonable parameter values, the riskfree rate effect would be larger than the risk premium effect. Thus recursive utility is needed to match the level of realized volatility itself. However, there is an additional affect that is relevant for option pricing. Drechsler and Yaron (2011) note that recursive utility implies a premium for volatility. Assets that fall in price when volatility rises are hedges and thus

---

<sup>14</sup>Backus, Chernov, and Martin (2011) write: “The question is whether the kinds of time dependence we see in asset prices are quantitatively important in assessing the role of extreme events. It is hard to make a definitive statement without knowing the precise form of time dependence, but there is good reason to think its impact could be small. The leading example in this context is stochastic volatility, a central feature of the option-pricing model estimated by Broadie et al. (2007). However, average implied volatility smiles from this model are very close to those from an iid model in which the variance is set equal to its mean. Furthermore, stochastic volatility has little impact on the probabilities of tail events, which is our interest here.”

have higher equilibrium prices than they would otherwise. Options are such an asset. We see the same mechanism in our model, except that it works through the channel of disaster risk. Indeed, an increase in the probability of a rare disaster raises option prices, while at the same time increasing marginal utility. Thus options are a hedge, which raises their prices, and thus raises implied volatilities.

The hedging property of options is quantitatively important. We can see this by replacing the pricing kernel in (10) with a fictitious one in which  $b_\lambda = 0$  (note that  $b_\xi = 0$  because we are starting with the single-frequency model).<sup>15</sup> Because  $b_\lambda$  determines the risk premium due to covariance with  $\lambda_t$ , setting  $b_\lambda = 0$  will shut off the hedging effect. Note that the assumption of  $b_\lambda = 0$  does not imply an iid model. This model still assumes that stock prices are driven by stochastic disaster risk; otherwise the volatility of stock returns would be equal to that of dividends. As Figure 4 shows, setting  $b_\lambda = 0$  reduces the level of implied volatilities so that it is noticeably below that of the data.

### 3.4 Alternative mechanisms

While it is not the purpose of this article to rule out all other possible explanations, here, we briefly discuss alternative models that could potentially explain the volatility skew.

Backus, Chernov, and Martin (2011) propose one such alternative mechanism, namely, that the consumption growth distribution is characterized by smaller and more negative jumps than in the disaster literature. This distribution is consistent with average implied volatilities as well as with the equity premium, and the mean and volatility of consumption

---

<sup>15</sup>Note that  $a$  also depends on  $b_\lambda$ : these expressions are also changed in the experiment. While it may first appear that  $b_\lambda$  should also affect the riskfree rate, this does not occur in the model with EIS=1. The riskfree rate satisfies a simple expression

$$r_t = \beta + \mu - \gamma\sigma^2 + \lambda_t E_\nu [e^{-\gamma Z} (e^Z - 1)].$$

growth observed in the U.S. in the 1889-2009 period (provided a coefficient of relative risk aversion equal to 8.7). However, this consumption distribution can be ruled out based on the history of consumption itself. Because it assumes that negative consumption jumps are relatively frequent (as they must be to explain the equity premium), some would have occurred in the 60-year postwar period in the U.S. The unconditional volatility of consumption growth in the U.S. during this period was less than 2%. Under the option-implied consumption growth distribution, there is less than a 1 in one million chance of observing a 60-year period with volatility this low.<sup>16</sup>

What about alternative modifications to the consumption distribution? In light of the discussion in Section 3.3, one such modification would be to allow volatility in consumption to be stochastic. This could generate variation in risk premia on equities, thus contributing to stock price volatility. However, consumption volatility does not appear to vary enough to explain equity volatility, nor does the resulting economy deviate sufficiently from unconditional normality to explain the slope of the volatility skew (additional details available from the authors upon request). In fact, the existing literature has explored rich models of consumption dynamics that include time-varying volatility (see Benzoni, Collin-Dufresne, and Goldstein (2011), Buraschi and Jiltsov (2006) and Drechsler (2013)). These papers find that, while the mechanism can capture deviations from the Black-Scholes benchmark, it is insufficient to match the extent of the deviation as measured by the skew in the data. Even models that can generate sufficient stock price volatility can fail to explain the skew. Du (2011) shows that the Campbell and Cochrane (1999) model alone does not explain option prices, though it can when augmented with iid rare events.

Other models that can quantitatively explain implied volatilities do so by making non-

---

<sup>16</sup>There are multiple additional objections to an iid model for returns. Another that arises in the context of options and rare disaster is that of Neuberger (2012), who shows that an iid model is unlikely based on the lack of decay in return skewness as the measurement horizon grows. We discuss this result further in Section 4.3.

standard assumptions on utilities or beliefs. For example, Drechsler (2013) assumes ambiguity aversion and Shaliastovich (2015) assumes jumps in confidence. These papers build on earlier work (Bates (2008), Liu, Pan, and Wang (2005)) that shows that crash aversion or ambiguity aversion is necessary to reconcile option prices and equity prices in the context of an iid model. One way to characterize this literature is that models that can explain the equity premium (or, in the case of dynamic models, the equity premium and volatility) can have difficulty explaining options without the addition of non-standard preferences or beliefs. The present model is an exception.

## 4 Option prices in a multifrequency stochastic disaster risk model

### 4.1 Why multiple frequencies?

The previous section shows that a model with stochastic disaster risk can explain average implied volatilities. To show this result, it suffices to use a simple model for the rare disaster probability in which a single state variable follows a square-root process.

However, closer examination suggests that this model may be overly restrictive. Figure 5 shows implied volatilities for  $\lambda_t$  equal to the median and for the 20th and 80th percentile value for put options with moneyness as low as 0.85. Implied volatilities increase almost in parallel as  $\lambda_t$  increases. That is, ATM options are affected by an increase in the rare disaster probability almost as much as out-of-the-money options. The model therefore implies that there should be little variation in the slope of the implied volatility curve.

Figure 6 shows the historical time series of implied volatilities computed on one month ATM and OTM options with moneyness of 0.85. Panel C shows the difference in the implied volatilities, a measure of the slope of the volatility skew. Defined in this way, the average

slope is 12%, with a volatility of 2%. Moreover, the slope can rise as high as 18% and fall as low as 6%. While the SDR model can explain the average slope, it seems unlikely that it would be able to account for the time-variation in the slope, at least under the current calibration. Moreover, comparing Panel C with Panels A and B of Figure 6 indicates that the slope varies independently of the level of implied volatilities. Thus it is unlikely that any model with a single state variable could account for these data.<sup>17</sup>

The mechanism in the SDR model that causes time-variation in rare disaster probabilities is identical to the mechanism that leads to volatility in normal times. Namely, when  $\lambda_t$  is high, rare disasters are more likely *and* returns are more volatile. In order to account for the data, a model must somehow decouple the volatility of stock returns from the probability of rare events. This is challenging, because volatility endogenously depends on the probability of rare events. Indeed, the main motivation for assuming time-variation in the probability of rare events is to generate volatility in stock returns that seems otherwise puzzling. Developing such a model is our goal in this section of the paper.<sup>18</sup>

## 4.2 Calibration

For simplicity, we keep risk aversion  $\gamma$ , the discount rate  $\beta$  and the leverage parameter  $\phi$  the same as in the single frequency SDR model. We also keep the distribution of consumption in the event of a disaster the same. Note that  $\kappa_\lambda$  and  $\sigma_\lambda$  will not have the same interpretation in the multifrequency model as  $\kappa$  and  $\sigma_\lambda$  do in the single frequency model.

Our first goal in calibrating the multifrequency model is to generate reasonable predictions for the aggregate market and for the consumption distribution. That is, we do not

---

<sup>17</sup>Christoffersen and Jacobs (2004) make this point in the context of reduced-form models.

<sup>18</sup>One might think that introducing time-variation in, say, the volatility of consumption growth would accomplish the same task. However, the problem is the same as that discussed in Section 3.4: the volatility in consumption growth does not vary nearly enough (at least at the relevant frequency) to generate variance in the slope independent of the level.

want to allow the probability of a disaster to become too high. One challenge in calibrating representative agent models is to match the high volatility of the price-dividend ratio. In the multifrequency model, as in the single frequency model, there is an upper limit to the amount of volatility that can be assumed in the state variable before a solution for utility fails to exist. The more persistent the processes, namely the lower the values of  $\kappa_\lambda$  and  $\kappa_\xi$ , the lower the respective volatilities must be so as to ensure that the discriminants in (8) and (9) stay nonnegative. We choose parameters so that the discriminant is equal to zero; thus there is only one more free parameter relative to the single-frequency model.

The resulting parameter choices are shown in Table 2. The mean reversion parameter  $\kappa_\lambda$  and volatility parameter  $\sigma_\lambda$  are relatively high, indicating a fast-moving component to the  $\lambda_t$  process, while the mean reversion parameter  $\kappa_\xi$  and  $\sigma_\xi$  are relatively low, indicating a slower-moving component. The parameter  $\bar{\xi}$  (which represents both the average value of  $\xi_t$  and the average value of  $\lambda_t$ ) is 2% per annum. This is lower than  $\bar{\lambda}$  in our calibration of the single-frequency model. In this sense, the multifrequency calibration is more conservative. However, the extra persistence created by the  $\xi_t$  process implies that  $\lambda_t$  could deviate from its average for long periods of time. To clarify the implications of these parameter choices, we report population statistics on  $\lambda_t$  in Panel C of Table 2. The median disaster probability is only 0.37%, indicating a highly skewed distribution. The standard deviation is 3.9% and the monthly first-order autocorrelation is 0.9858.

Implications for the riskfree rate and the market are shown in Table 3. We simulate 100,000 samples of length 60 years to capture features of the small-sample distribution. We also simulate a long sample of 600,000 years to capture the population distribution. Statistics are reported for the full set of 100,000 samples, and the subset for which there are no disasters (38% of the sample paths). The table reveals a good fit to the equity premium and to return volatility. The average Treasury Bill rate is slightly too high, though this could be lowered

by lowering  $\beta$  or by lowering the probability of government default.<sup>19</sup> The model successfully captures the low volatility of the riskfree rate in the postwar period. The model matches the equity premium well, with a median value for no-disaster simulations of 8% (compared with the data value of 7.3%).<sup>20</sup> The model also matches equity volatility; the median is 19.3%, compared with a data value of 17.8%. Like other models of this type (see, e.g. Bansal and Yaron (2004), Bansal, Kiku, and Yaron (2012)), the volatility of the price-dividend ratio is somewhat below its value in the data (0.27 versus 0.43). However, the data value is still lower than the 95th percentile among the simulated samples.<sup>21</sup> For the market moments, only the very high AR(1) coefficient in postwar data falls outside the 90% confidence bounds: it is 0.92 (annual), while in the data, the median is 0.79 and the 95th percentile value is 0.91. While it is theoretically possible to match this autocorrelation in the model, it comes at a cost of raising the autocorrelation of option prices beyond realistic levels. Moreover, so that utility converges, there is a tradeoff between persistence and volatility. One view is that the autocorrelation of the price-dividend ratio observed in the postwar period may in fact have been very exceptional and perhaps is not a moment that should be targeted too stringently.

### 4.3 Implied volatilities in the multifrequency model

We first examine the fit of the model to the mean of implied volatilities in the data. We consider implied volatilities at a wider range of moneyness; we also look at 1- and 6-month options as well as 3-month options and we consider the second moment of implied volatilities as well as the first moment. Finally, rather than looking only at the population average,

---

<sup>19</sup>As in the single frequency model, we assume a 40% probability of government default.

<sup>20</sup>The population value of the equity premium is higher, at 9%. However, the no-disaster median is the more relevant number of comparison with postwar data. The no-disaster median is lower because, on average, the disaster probability is lower in samples without disasters.

<sup>21</sup>The single-frequency model, which was calibrated to match the population persistence of the price-dividend ratio, has a median price-dividend ratio volatility of 0.21 for sample paths without disasters and a population price-dividend ratio volatility of 0.38.

we consider the range of values we would see in repeated samples that resemble the data, namely, samples of length 17 years with no disaster. This is a similar exercise to what was performed in Table 3, though calculating option prices is technically more difficult than calculating equity prices.<sup>22</sup>

Figure 7 shows means and volatilities of implied volatilities for the three option maturities. We report the averages across each sample path, as well as 90% confidence intervals from the simulation. We see that this new model is successful at matching the average level of the implied volatility curve for all three maturities, even with this extended moneyness range, and even though we are looking at sample paths in which the disaster probability will be lower than average. In fact the slope in the model is slightly below that in the data. Similarly, the model's predictions for volatility of volatility are well within the standard error bars for all moneyness levels and for all three option maturities.<sup>23</sup>

The volatility skew computed from options expiring in as long as six months indicates that the risk-neutral distribution of returns exhibits considerable skewness at long horizons. This is known as the skewness puzzle (Bates (2008)) because the law of large numbers would suggest convergence toward normality as the time to expiration increases. Recently, Neuberger (2012) makes use of options data to conclude that the skewness in the physical distribution of

---

<sup>22</sup>Because of the extra persistence in the multifrequency model,  $\lambda_t$  spends more time near zero. To accurately capture the dynamics when  $\lambda_t$  is near zero, we simulate the model at a half-day interval for 17 years. This simulation is repeated 1000 times for the options calculation, and more for the (easier) equity calculations. Along each simulation path, we pick monthly observations of the state variables and calculate option prices for these monthly observations. Given the values of the state variables, the log-linear approximation is equally accurate as in the single-frequency model.

<sup>23</sup>One issue that arises in fitting both options and equities with a single model is the very different levels of persistence in the option and equity markets. As Table 3 reports, the annual AR(1) coefficient for the price-dividend ratio in the data is extremely high: 0.92; just outside of our 10% confidence intervals. The median value from the simulations is still a very high 0.79; in monthly simulations, this value is 0.98. Implied volatilities in simulated data have much lower autocorrelations. Median autocorrelations are roughly the same across moneyness levels, and are in the 0.92 to 0.94 range; substantially below the level for the price-dividend ratio. The AR(1) coefficients in the data are lower still, though generally within the 10% confidence intervals. While the same state variables drive equity and option prices, they do so to different extents. The model endogenously captures the greater persistence in equity prices, which represent value in the longer run than do option prices.

returns is also more pronounced than has been estimated previously. Neuberger emphasizes the observed negative correlation between stock prices and volatility (French, Schwert, and Stambaugh (1987)) as a reason why skewness in long-horizon returns does not decay as the law of large numbers in an iid model suggests that it would (see also Bates (2000)).

Figure 7 shows that our model can capture the downward slope in 6-month implied volatilities as well as the slope for shorter-term options. Thus stock returns in the model exhibit skewness at both long and short-horizons. The short-horizon skewness arises from the existence of rare disasters. Long-horizon skewness, however, comes about endogenously because of the time-variation in the disaster probability. An increase in the rare disaster probability leads to lower stock prices, and, at the same time, higher volatilities, thereby accounting for this co-movement in the data. As a result, returns maintain their skewness at long horizons, and the model can explain six-month as well as one-month implied volatility curves.

#### **4.4 Slope of the implied volatility skew**

We now return to the question we posed at the beginning of this section. Does this model explain variation in the slope of the volatility skew, and, if so, how does it do this?

As in the previous section, we simulate 1000 samples of length 17 years from the multi-frequency SDR model, retaining only those with no disasters. For each simulation path, we calculate the mean and the volatility of the difference between the OTM and ATM implied volatilities. Figure 8 shows a scatter plot of these means and volatilities, along with the value in the data, represented by circles. For comparison, we repeat this exercise for the single-frequency SDR model (represented by squares). We also show the value for the CDR model. Because the CDR model is iid, any simulation will generate an identical volatility skew, and so the CDR model is represented by a single point (a triangle). Moreover, there

is zero variance in the CDR volatility skew.

Confirming the results from Section 3, Figure 8 shows that the volatility skew in the CDR model is much larger than the average volatility skew in the data. Much closer to the data is the average volatility skew for the SDR model. However, as discussed above, the single-frequency model predicts that the volatility in the volatility skew is close to zero. The multifrequency model is closer to the data along both the mean and volatility dimensions. Unlike the single-frequency model, the data fall within the 95 percent confidence ellipse implied by the model.

Why does the multifrequency model succeed in producing independent variation in the slope and level of the volatility skew? Figure 9 shows how each state variable affects the volatility skew: in Panel A we vary  $\lambda_t$  while holding  $\xi_t$  at its median, while in Panel B we vary  $\xi_t$ , holding  $\lambda_t$  at its median. As expected, both variables impact both the ATM and OTM options. However,  $\lambda_t$  has a greater effect on OTM options, which is intuitive, as  $\lambda_t$  directly measures the disaster probability. On the other hand,  $\xi_t$  has a larger effect on ATM options, because of its impact on volatility.

## 4.5 The time series of options and equities

We now ask what these implied volatilities say about equity valuations.

We consider the time series of one-month ATM and OTM implied volatilities (Figure 6). For each of these data points, we compute the implied value of  $\lambda_t$  and  $\xi_t$ . Note that this exercise would not be possible if the model were not capable of simultaneously matching the level and slope of the implied volatility curve for one-month options.<sup>24</sup> Before embarking on this exercise we note that the matching the time series is not usually a target for general equilibrium models because these models operate under tight constraints. We expect that

---

<sup>24</sup>The resulting time series provides an excellent fit to the time-series of 3 and 6-month options, suggesting that the choice of 1-month options is not important for this exercise.

there will be some aspects of the time series that our model will not be able to match.

Given the option-implied values of  $\xi$  and  $\lambda$ , we can impute a price-dividend ratio using (12). This price-dividend ratio uses no data on equities, only data on options and the model. Figure 10 shows the results, along with the price-dividend ratio from data available from Robert Shiller's webpage. The model can match the sustained level of the price-dividend ratio, and, most importantly, the time series variation after 2004.<sup>25</sup> Indeed, between 2004 and 2013, the correlation between the option-implied price-dividend ratio and the actual price-dividend ratio is 0.84, strongly suggesting these two markets share a common source of risk.

## 5 Conclusion

Since the early work of Rubinstein (1994), the volatility skew has constituted an important piece of evidence against the Black-Scholes Model, and a lens through which to view the success of a model in matching option prices.

The volatility skew, almost by definition, has been associated with excess kurtosis in stock prices. Separately, a literature has developed linking kurtosis in consumption (which would then be inherited by returns in equilibrium) with the equity premium. However, much of the work up to now suggests that, at least for standard preferences, the non-normalities required to match the equity premium are qualitatively different from those required to match implied volatility.

We have proposed an alternative and more general approach to modeling the risk of downward jumps that can reconcile the volatility skew and the equity premium. Rather than assuming that the probability of a large negative event is constant, we allow it to vary

---

<sup>25</sup>Not surprisingly, the disaster-risk model is not able to match the run-up in stock prices from the late 90s until around 2004. It may be that time-varying fears of a disaster will not be able to capture the extreme optimism that characterized that period.

over time. The existence of very bad consumption events leads to both the downward slope in the volatility skew and the equity premium. Moreover, the time-variation in these events moderates the slope, raises the level and generates the excess volatility observed in stock prices. Thus the model can simultaneously match the equity premium, equity volatility, and implied volatilities on index options. Option prices, far from ruling out rare consumption disasters, provide additional information for the existence of what has been referred to as the “dark matter” of asset pricing (Campbell (2008), Chen, Dou, and Kogan (2013)).

The initial model that we develop in the paper is deliberately simple and parsimonious. However, there are some interesting features of option and stock prices that cannot be matched by a model with a single state variable; for example, the imperfect correlation between the slope and the level of the volatility skew. For this reason, we investigate a more general model that allows for variation in disaster risk to occur at multiple time scales. This modification naturally produces time-variation in the slope of implied volatilities because it introduces variation in stock price volatility that can be distinguished from the risk of rare disasters. Taken together, these results indicate that options data support the existence of rare disasters in beliefs about the equity premium. Moreover, options data can provide information about the disaster distribution beyond that offered by stock prices. In particular, data from options suggest that modeling time-variation in disaster risk occurring at multiple time scales may be a fruitful avenue for future work.

# Appendix

## A Data construction

Our sample consists of daily data on option prices, volume and open interest for European put options on the S&P 500 index from OptionMetrics. Data are from 1996 to 2012. Options expire on the Saturday that follows the third Friday of the month. We extract monthly observations using data from the Wednesday of every option expiration week. We apply standard filters to ensure that the contracts on which we base our analyses trade sufficiently often for prices to be meaningful. That is, we exclude observations with bid price smaller than  $1/8$  and those with zero volume and open interest smaller than one hundred contracts (Shaliastovich (2009)).

OptionMetrics constructs implied volatilities using the formula of Black and Scholes (1973) (generalized for an underlying that pays dividends), with LIBOR as the short-term interest rate. The dividend-yield is extracted from the put-call parity relation. We wish to construct a data set of implied volatilities with maturities of 1, 3 and 6 months across a range of strike prices. Of course, there will not be liquid options with maturity precisely equal to, say, 3 months, at each date. For this reason, we use polynomial interpolation across strike prices and times to expiration.<sup>26</sup> Specifically, at each date in the sample, we regress implied volatilities on a polynomial in strike price  $K$  and maturity  $T$ :

$$\sigma(K, T) = \theta_0 + \theta_1 K + \theta_2 K^2 + \theta_3 T + \theta_4 T^2 + \theta_5 KT + \theta_6 KT^2 + \epsilon_{K,T}$$

We run this regression on options with maturities ranging from 30 to 247 days, and with moneyness below 1.1. The implied volatility surface is generated by the fitted values of this

---

<sup>26</sup>See Dumas, Fleming, and Whaley (1998), Christoffersen and Jacobs (2004) and Christoffersen, Heston, and Jacobs (2009).

regression.

## B Model Solution

### B.1 Utility

We conjecture that, in equilibrium, the continuation utility  $V_t$  equals a function  $J$  of consumption and the state variables  $\lambda$  and  $\xi$  such that:

$$J(C, \lambda, \xi) = \frac{C^{1-\gamma}}{1-\gamma} e^{a+b_\lambda\lambda+b_\xi\xi}. \quad (\text{B.1})$$

By differentiating  $J(C, \lambda, \xi)$ , we obtain

$$\begin{aligned} \frac{\partial J}{\partial C} &= (1-\gamma)\frac{J}{C}, & \frac{\partial^2 J}{\partial C^2} &= -\gamma(1-\gamma)\frac{J}{C^2}, \\ \frac{\partial J}{\partial \lambda} &= b_\lambda J, & \frac{\partial^2 J}{\partial \lambda^2} &= b_\lambda^2 J, \\ \frac{\partial J}{\partial \xi} &= b_\xi J, & \frac{\partial^2 J}{\partial \xi^2} &= b_\xi^2 J. \end{aligned} \quad (\text{B.2})$$

Applying Ito's Lemma to  $J(C, \lambda, \xi)$  with conjecture (B.1) and derivatives (B.2):

$$\begin{aligned} \frac{dV_t}{V_t^-} &= (1-\gamma)(\mu dt + \sigma dB_t) - \frac{1}{2}\gamma(1-\gamma)\sigma^2 dt \\ &\quad + b_\lambda \left( \kappa_\lambda(\xi_t - \lambda_t)dt + \sigma_\lambda \sqrt{\lambda_t} dB_{\lambda,t} \right) + \frac{1}{2}b_\lambda^2 \sigma_\lambda^2 \lambda_t dt \\ &\quad + b_\xi \left( \kappa_\xi(\bar{\xi} - \xi_t)dt + \sigma_\xi \sqrt{\xi_t} dB_{\xi,t} \right) + \frac{1}{2}b_\xi^2 \sigma_\xi^2 \xi_t dt + (e^{(1-\gamma)Z_t} - 1)dN_t. \end{aligned}$$

Under the optimal consumption path, it must be that

$$V_t + \int_0^t f(C_s, V_s) ds = E_t \left[ \int_0^\infty f(C_s, V_s) ds \right] \quad (\text{B.3})$$

(see Duffie and Epstein (1992)). By definition,

$$\begin{aligned}
f(C, V) &= \beta(1 - \gamma)V \left( \log C - \frac{1}{1 - \gamma} \log [(1 - \gamma)V] \right) \\
&= \beta(1 - \gamma)V \log C - \beta V \log [(1 - \gamma)V] \\
&= \beta V \log \left( \frac{C^{1-\gamma}}{(1 - \gamma)V} \right) \\
&= -\beta V(a + b_\lambda \lambda + b_\xi \xi),
\end{aligned} \tag{B.4}$$

where the last equation follows from the equilibrium condition that the utility process is equal to the value function under the optimal policies:  $V_t = J(C_t, \lambda_t, \xi_t)$ .

By the law of iterative expectations, the left-hand side of (B.3) is a martingale. Thus, the sum of the drift and the jump compensator of  $(V_t + \int_0^t f(C_s, V_s) ds)$  equals zero. That is,

$$\begin{aligned}
0 = (1 - \gamma)\mu - \frac{1}{2}\gamma(1 - \gamma)\sigma^2 + b_\lambda \kappa_\lambda (\xi_t - \lambda_t) + \frac{1}{2}b_\lambda^2 \sigma_\lambda^2 \lambda_t + b_\xi \kappa_\xi (\bar{\xi} - \xi_t) + \frac{1}{2}b_\xi^2 \sigma_\xi^2 \xi_t \\
+ \lambda_t E_\nu [e^{(1-\gamma)Z_t} - 1] - \beta(a + b_\lambda \lambda_t + b_\xi \xi_t). \tag{B.5}
\end{aligned}$$

By collecting terms in (B.5), we obtain

$$\begin{aligned}
0 = & \underbrace{\left[ (1 - \gamma)\mu - \frac{1}{2}\gamma(1 - \gamma)\sigma^2 + b_\xi \kappa_\xi \bar{\xi} - \beta a \right]}_{=0} \\
& + \lambda_t \underbrace{\left[ -b_\lambda \kappa_\lambda + \frac{1}{2}b_\lambda^2 \sigma_\lambda^2 + E_\nu [e^{(1-\gamma)Z_t} - 1] - \beta b_\lambda \right]}_{=0} \\
& + \xi_t \underbrace{\left[ b_\lambda \kappa_\lambda - b_\xi \kappa_\xi + \frac{1}{2}b_\xi^2 \sigma_\xi^2 - \beta b_\xi \right]}_{=0}. \tag{B.6}
\end{aligned}$$

Solving these equations gives us

$$a = \frac{1-\gamma}{\beta} \left( \mu - \frac{1}{2} \gamma \sigma^2 \right) + \frac{b_\xi \kappa_\xi \bar{\xi}}{\beta} \quad (\text{B.7})$$

$$b_\lambda = \frac{\kappa_\lambda + \beta}{\sigma_\lambda^2} - \sqrt{\left( \frac{\kappa_\lambda + \beta}{\sigma_\lambda^2} \right)^2 - 2 \frac{E_\nu [e^{(1-\gamma)Z_t} - 1]}{\sigma_\lambda^2}} \quad (\text{B.8})$$

$$b_\xi = \frac{\kappa_\xi + \beta}{\sigma_\xi^2} - \sqrt{\left( \frac{\kappa_\xi + \beta}{\sigma_\xi^2} \right)^2 - 2 \frac{b_\lambda \kappa_\lambda}{\sigma_\xi^2}}, \quad (\text{B.9})$$

where we have chosen the negative root based on the economic consideration that when there are no disasters,  $\lambda_t$  and  $\xi_t$  should not appear in the value function. Namely, for  $Z_t = 0$ ,  $b_\lambda = b_\xi = 0$ . Lastly, note that these results verify the conjecture (B.1).

## B.2 State-price density

Duffie and Skiadas (1994) show that the state-price density  $\pi_t$  equals

$$\pi_t = \exp \left\{ \int_0^t \frac{\partial}{\partial V} f(C_s, V_s) ds \right\} \frac{\partial}{\partial C} f(C_t, V_t). \quad (\text{B.10})$$

Our goal is to obtain an expression for the state-price density in terms of  $C_t$ ,  $\lambda_t$  and  $\xi_t$ .

It follows from (B.4) that

$$\frac{\partial}{\partial C} f(C_t, V_t) = \beta C_t^{-\gamma} e^{a+b_\lambda \lambda_t + b_\xi \xi_t}$$

and

$$\frac{\partial}{\partial V} f(C_t, V_t) = \beta(1-\gamma) \left( \log C_t - \frac{1}{1-\gamma} \log((1-\gamma)V_t) \right) + \beta.$$

In equilibrium, continuation value  $V_t = J(C_t, \lambda_t, \xi_t)$ . Substituting in for  $V_t$  from (B.1) implies

$$\frac{\partial}{\partial V} f(C_t, V_t) = -\beta a - \beta - \beta b_\lambda \lambda_t - \beta b_\xi \xi_t. \quad (\text{B.11})$$

Therefore, from (B.10), it follows that the state-price density can be written as

$$\pi_t = \exp \left\{ -\beta(a+1)t - \beta b_\lambda \int_0^t \lambda_s ds - \beta b_\xi \int_0^t \xi_s ds \right\} \beta C_t^{-\gamma} e^{a+b_\lambda \lambda_t + b_\xi \xi_t}. \quad (\text{B.12})$$

### B.3 Dividend claim price

Let  $F_t$  denote the price of the dividend claim. The pricing relation implies

$$\begin{aligned} F_t &= E_t \left[ \int_t^\infty \frac{\pi_s}{\pi_t} D_s ds \right] \\ &= \int_t^\infty E_t \left[ \frac{\pi_s}{\pi_t} D_s \right] ds. \end{aligned}$$

Let  $H(D_t, \lambda_t, \xi_t, s-t)$  denote the price of the asset that pays the aggregate dividend at time  $s$ , namely,

$$H(D_t, \lambda_t, \xi_t, s-t) = E_t \left[ \frac{\pi_s}{\pi_t} D_s \right].$$

By the law of iterative expectations, it follows that  $\pi_t H_t$  is a martingale:

$$\pi_t H(D_t, \lambda_t, \xi_t, s-t) = E_t[\pi_s D_s].$$

Conjecture that

$$H(D_t, \lambda_t, \xi_t, \tau) = D_t \exp(a_\phi(\tau) + b_{\phi\lambda}(\tau)\lambda_t + b_{\phi\xi}(\tau)\xi_t). \quad (\text{B.13})$$

Define  $\mu_D$  to be the drift rate of the dividend process. By Ito's Lemma applied to the definition of dividends, it follows that

$$\mu_D = \phi\mu + \frac{1}{2}\phi(\phi - 1)\sigma^2.$$

Applying Ito's Lemma to the conjecture implies

$$\begin{aligned} \frac{dH_t}{H_{t-}} = & \left\{ \mu_D + b_{\phi\lambda}(\tau)\kappa_\lambda(\xi_t - \lambda_t) + \frac{1}{2}b_{\phi\lambda}(\tau)^2\sigma_\lambda^2\lambda_t + b_{\phi\xi}(\tau)\kappa_\xi(\bar{\xi} - \xi_t) + \frac{1}{2}b_{\phi\xi}(\tau)^2\sigma_\xi^2\xi_t \right. \\ & \left. - a'_\phi(\tau) - b'_{\phi\lambda}(\tau)\lambda_t - b'_{\phi\xi}(\tau)\xi_t \right\} dt \\ & + \phi\sigma dB_t + b_{\phi\lambda}(\tau)\sigma_\lambda\sqrt{\lambda_t}dB_{\lambda,t} + b_{\phi\xi}(\tau)\sigma_\xi\sqrt{\xi_t}dB_{\xi,t} + (e^{\phi Z_t} - 1)dN_t. \end{aligned}$$

Combining the SDE for  $H_t$  with the one for  $\pi_t$  derived in the previous sections, we can derive the SDE for  $\pi_t H_t$ :

$$\begin{aligned} \frac{d(\pi_t H_t)}{\pi_{t-} H_{t-}} = & \left\{ -\beta - \mu + \gamma\sigma^2 - \lambda_t E_\nu [e^{(1-\gamma)Z_t} - 1] \right. \\ & + \mu_D + b_{\phi\lambda}(\tau)\kappa_\lambda(\xi_t - \lambda_t) + \frac{1}{2}b_{\phi\lambda}(\tau)^2\sigma_\lambda^2\lambda_t \\ & + b_{\phi\xi}(\tau)\kappa_\xi(\bar{\xi} - \xi_t) + \frac{1}{2}b_{\phi\xi}(\tau)^2\sigma_\xi^2\xi_t \\ & - a'_\phi(\tau) - b'_{\phi\lambda}(\tau)\lambda_t - b'_{\phi\xi}(\tau)\xi_t \\ & \left. - \gamma\phi\sigma^2 + b_\lambda b_{\phi\lambda}(\tau)\sigma_\lambda^2\lambda_t + b_\xi b_{\phi\xi}(\tau)\sigma_\xi^2\xi_t \right\} dt \\ & + (\phi - \gamma)\sigma dB_t + (b_\lambda + b_{\phi\lambda}(\tau))\sigma_\lambda\sqrt{\lambda_t}dB_{\lambda,t} + (b_\xi + b_{\phi\xi}(\tau))\sigma_\xi\sqrt{\xi_t}dB_{\xi,t} \\ & + (e^{(\phi-\gamma)Z_t} - 1)dN_t. \end{aligned}$$

Since  $\pi_t H_t$  is a martingale, the sum of the drift and the jump compensator of  $\pi_t H_t$  equals zero. Thus:

$$\begin{aligned}
0 = & -\beta - \mu + \gamma\sigma^2 - \lambda_t E_\nu [e^{(1-\gamma)Z_t} - 1] \\
& + \mu_D + b_{\phi\lambda}(\tau)\kappa_\lambda(\xi_t - \lambda_t) + \frac{1}{2}b_{\phi\lambda}(\tau)^2\sigma_\lambda^2\lambda_t \\
& + b_{\phi\xi}(\tau)\kappa_\xi(\bar{\xi} - \xi_t) + \frac{1}{2}b_{\phi\xi}(\tau)^2\sigma_\xi^2\xi_t \\
& - a'_\phi(\tau) - b'_{\phi\lambda}(\tau)\lambda_t - b'_{\phi\xi}(\tau)\xi_t \\
& - \gamma\phi\sigma^2 + b_\lambda b_{\phi\lambda}(\tau)\sigma_\lambda^2\lambda_t + b_\xi b_{\phi\xi}(\tau)\sigma_\xi^2\xi_t + \lambda_t E_\nu [e^{(\phi-\gamma)Z_t} - 1]. \quad (\text{B.14})
\end{aligned}$$

Collecting terms of (B.14) results in the following equation:

$$\begin{aligned}
0 = & \underbrace{[-\beta - \mu + \gamma\sigma^2 + \mu_D + b_{\phi\xi}(\tau)\kappa_\xi\bar{\xi} - \gamma\phi\sigma^2 - a'_\phi(\tau)]}_{=0} \\
& + \lambda_t \underbrace{\left[ -b_{\phi\lambda}(\tau)\kappa_\lambda + \frac{1}{2}b_{\phi\lambda}(\tau)^2\sigma_\lambda^2 + b_\lambda b_{\phi\lambda}(\tau)\sigma_\lambda^2 + E_\nu [e^{(\phi-\gamma)Z_t} - e^{(1-\gamma)Z_t}] - b'_{\phi\lambda}(\tau) \right]}_{=0} \\
& + \xi_t \underbrace{\left[ b_{\phi\lambda}(\tau)\kappa_\lambda - b_{\phi\xi}(\tau)\kappa_\xi + \frac{1}{2}b_{\phi\xi}(\tau)^2\sigma_\xi^2 + b_\xi b_{\phi\xi}(\tau)\sigma_\xi^2 - b'_{\phi\xi}(\tau) \right]}_{=0}.
\end{aligned}$$

It follows that

$$\begin{aligned}
a'_\phi(\tau) &= \mu_D - \mu - \beta + \gamma\sigma^2(1 - \phi) + \kappa_\xi\bar{\xi}b_{\phi\xi}(\tau) \\
b'_{\phi\lambda}(\tau) &= \frac{1}{2}\sigma_\lambda^2 b_{\phi\lambda}(\tau)^2 + (b_\lambda\sigma_\lambda^2 - \kappa_\lambda)b_{\phi\lambda}(\tau) + E_\nu [e^{(\phi-\gamma)Z_t} - e^{(1-\gamma)Z_t}] \quad (\text{B.15}) \\
b'_{\phi\xi}(\tau) &= \frac{1}{2}\sigma_\xi^2 b_{\phi\xi}(\tau)^2 + (b_\xi\sigma_\xi^2 - \kappa_\xi)b_{\phi\xi}(\tau) + \kappa_\lambda b_{\phi\lambda}(\tau).
\end{aligned}$$

This establishes that  $H$  satisfies the conjecture (B.13). We note that by no-arbitrage,

$$H(D_t, \lambda_t, \xi_t, 0) = D_t.$$

This condition provides the boundary conditions for the system of ODEs (B.15):

$$a_\phi(0) = b_{\phi\lambda}(0) = b_{\phi\xi}(0) = 0.$$

Recall that once we get  $a_\phi(\tau)$ ,  $b_{\phi\lambda}(\tau)$ , and  $b_{\phi\xi}(\tau)$ ,

$$\begin{aligned} F_t &= \int_t^\infty E_t \left[ \frac{\pi_s}{\pi_t} D_s \right] ds \\ &= \int_t^\infty H(D_t, \lambda_t, \xi_t, s-t) ds \\ &= D_t \int_t^\infty \exp(a_\phi(s-t) + b_{\phi\lambda}(s-t)\lambda_t + b_{\phi\xi}(s-t)\xi_t) ds \\ &= D_t \int_0^\infty \exp(a_\phi(\tau) + b_{\phi\lambda}(\tau)\lambda_t + b_{\phi\xi}(\tau)\xi_t) d\tau. \end{aligned}$$

That is, the price-dividend ratio can be written as

$$G(\lambda_t, \xi_t) = \int_0^\infty \exp(a_\phi(\tau) + b_{\phi\lambda}(\tau)\lambda_t + b_{\phi\xi}(\tau)\xi_t) d\tau.$$

#### B.4 Approximating the price-dividend ratio to obtain option prices

The transform analysis we use to price options requires that the log of the price-dividend ratio be linear. Fortunately, the exact price-dividend ratio we derive can be closely approximated by a log-linear function.

Let  $g(\lambda, \xi) = \log G(\lambda, \xi)$ . For given  $\lambda^*$  and  $\xi^*$ , the two-dimensional Taylor approximation

implies

$$g(\lambda, \xi) \simeq g(\lambda^*, \xi^*) + \left. \frac{\partial g}{\partial \lambda} \right|_{\lambda^*, \xi^*} (\lambda - \lambda^*) + \left. \frac{\partial g}{\partial \xi} \right|_{\lambda^*, \xi^*} (\xi - \xi^*). \quad (\text{B.16})$$

We note that

$$\begin{aligned} \left. \frac{\partial g}{\partial \lambda} \right|_{\lambda^*, \xi^*} &= \frac{1}{G(\lambda^*, \xi^*)} \left. \frac{\partial G}{\partial \lambda} \right|_{\lambda^*, \xi^*} \\ &= \frac{1}{G(\lambda^*, \xi^*)} \int_0^\infty b_{\phi\lambda}(\tau) \exp(a_\phi(\tau) + b_{\phi\lambda}(\tau)\lambda^* + b_{\phi\xi}(\tau)\xi^*) d\tau \end{aligned} \quad (\text{B.17})$$

Similarly, we obtain

$$\begin{aligned} \left. \frac{\partial g}{\partial \xi} \right|_{\lambda^*, \xi^*} &= \frac{1}{G(\lambda^*, \xi^*)} \left. \frac{\partial G}{\partial \xi} \right|_{\lambda^*, \xi^*} \\ &= \frac{1}{G(\lambda^*, \xi^*)} \int_0^\infty b_{\phi\xi}(\tau) \exp(a_\phi(\tau) + b_{\phi\lambda}(\tau)\lambda^* + b_{\phi\xi}(\tau)\xi^*) d\tau. \end{aligned} \quad (\text{B.18})$$

Expression (B.17) and (B.18) can be interpreted as weighted averages of the coefficients  $b_{\phi\lambda}(\tau)$  and  $b_{\phi\xi}(\tau)$  respectively. The average is over  $\tau$ , and the weights are proportional to  $\exp\{a_\phi(\tau) + b_{\phi\lambda}(\tau)\lambda^* + b_{\phi\xi}(\tau)\xi^*\}$ . With this in mind, we define the notation

$$b_{\phi\lambda}^* = \frac{1}{G(\lambda^*, \xi^*)} \int_0^\infty b_{\phi\lambda}(\tau) \exp(a_\phi(\tau) + b_{\phi\lambda}(\tau)\lambda^* + b_{\phi\xi}(\tau)\xi^*) d\tau \quad (\text{B.19})$$

$$b_{\phi\xi}^* = \frac{1}{G(\lambda^*, \xi^*)} \int_0^\infty b_{\phi\xi}(\tau) \exp(a_\phi(\tau) + b_{\phi\lambda}(\tau)\lambda^* + b_{\phi\xi}(\tau)\xi^*) d\tau, \quad (\text{B.20})$$

and the log-linear function

$$\hat{G}(\lambda_t, \xi_t) = G(\lambda^*, \xi^*) \exp\{b_{\phi\lambda}^*(\lambda_t - \lambda^*) + b_{\phi\xi}^*(\xi_t - \xi^*)\}. \quad (\text{B.21})$$

It follows from exponentiating both sides of (B.16) that

$$G(\lambda_t, \xi_t) \simeq \hat{G}(\lambda_t, \xi_t).$$

In our analysis, we pick  $\lambda^*$  and  $\xi^*$  as the stationary mean of  $\lambda_t$  and  $\xi_t$ , respectively.

This log-linearization method differs from the more widely-used method of Campbell (2003), applied in continuous time by Chacko and Viceira (2005). However, in this application it is more accurate. This is not surprising, since we are able to exploit the fact that the true solution for the price-dividend ratio is known. In dynamic models with the EIS not equal to one, the solution is typically unknown.

## C Derivation of Limiting Cases

### C.1 Single-frequency SDR as the limit of multifrequency SDR

Note that  $b_\xi$  in equation (B.9) can be written as

$$b_\xi = \frac{1}{\sigma_\xi^2} \left( \kappa_\xi + \beta - \sqrt{(\kappa_\xi + \beta)^2 - 2b_\lambda \kappa_\lambda \sigma_\xi^2} \right).$$

Applying L'Hopital's rule yields

$$\lim_{\sigma_\xi \rightarrow 0} b_\xi = \lim_{\sigma_\xi \rightarrow 0} \frac{1}{2} \left( (\kappa_\xi + \beta)^2 - 2b_\lambda \kappa_\lambda \sigma_\xi^2 \right)^{-\frac{1}{2}} 2b_\lambda \kappa_\lambda = \frac{b_\lambda \kappa_\lambda}{\kappa_\xi + b_\xi} \quad (\text{C.1})$$

It follows from the equation for  $a$ , (B.7), that

$$\begin{aligned}
\lim_{\sigma_\lambda \rightarrow 0} (a + b_\lambda \lambda_t + b_\xi \xi_t) &= \lim_{\sigma_\xi \rightarrow 0} (a + b_\xi \bar{\lambda} + b_\lambda \lambda_t) \\
&= \frac{1 - \gamma}{\beta} \left( \mu - \frac{1}{2} \gamma \sigma^2 \right) + \frac{b_\xi \kappa_\xi \bar{\lambda}}{\beta} + \bar{\lambda} \lim_{\sigma_\xi \rightarrow 0} b_\xi + b_\lambda \lambda_t \\
&= \frac{1 - \gamma}{\beta} \left( \mu - \frac{1}{2} \gamma \sigma^2 \right) + \frac{1}{\beta} b_\lambda \kappa_\lambda \bar{\lambda} + b_\lambda \lambda_t,
\end{aligned}$$

where we assume  $\xi_0 = \bar{\xi} \equiv \bar{\lambda}$  and apply (C.1).<sup>27</sup> Note that the limit of the stochastic process for consumption is given by (1), with

$$d\lambda_t = \kappa(\bar{\lambda} - \lambda_t) dt + \sigma_\lambda \sqrt{\lambda_t} dB_{\lambda,t}.$$

We now apply these results to calculate the limit of the state-price density  $\pi_t$ . For asset prices, all that matters are ratios of  $\pi_t$  at different points in time, so we normalize by  $\pi_0$ . From (B.12) it follows that

$$\begin{aligned}
\lim_{\sigma_\xi \rightarrow 0} \frac{\pi_t}{\pi_0} &= \exp \left\{ -\beta \left( \lim_{\sigma_\xi \rightarrow 0} (a + b_\xi \bar{\lambda}) t + b_\lambda \int_0^t \lambda_s ds \right) + b_\lambda \lambda_t \right\} \beta \left( \frac{C_t}{C_0} \right)^{-\gamma} \\
&= \exp \left\{ -\beta - (1 - \gamma) \left( \mu - \frac{1}{2} \gamma \sigma^2 \right) - b_\lambda \kappa_\lambda \bar{\lambda} - \beta b_\lambda \int_0^t \lambda_s ds + b_\lambda \lambda_t \right\} \beta \left( \frac{C_t}{C_0} \right)^{-\gamma}
\end{aligned}$$

This is the same state-price density as in Wachter (2013). Note that this result requires that we chose the lower of the two roots in (B.6).<sup>28</sup>

## C.2 CDR as the iid limit of the SDR model

We now further take the limit as  $\sigma_\lambda$  goes to zero to produce an iid model.

<sup>27</sup>This matches the expression in Wachter (2013), when adjusted for the fact that, in this paper, we express the value function in terms of wealth, whereas the previous paper expressed the value function in terms of consumption.

<sup>28</sup>This point is also made by Tauchen (2005) for a model with stochastic volatility.

Note that  $b_\lambda$  in equation (B.8) can be rewritten as

$$b_\lambda = \frac{1}{\sigma_\lambda^2} \left( \kappa_\lambda + \beta - \sqrt{(\kappa_\lambda + \beta)^2 - 2E_\nu [e^{(1-\gamma)Z} - 1] \sigma_\lambda^2} \right).$$

We take limits using L'Hopital's rule:

$$\begin{aligned} \lim_{\sigma_\lambda \rightarrow 0} b_\lambda &= \lim_{\sigma_\lambda \rightarrow 0} \frac{1}{2} \left( (\kappa_\lambda + \beta)^2 - 2E_\nu [e^{(1-\gamma)Z} - 1] \sigma_\lambda^2 \right)^{-\frac{1}{2}} 2E_\nu [e^{(1-\gamma)Z} - 1] \\ &= \frac{E_\nu [e^{(1-\gamma)Z} - 1]}{\kappa_\lambda + \beta}. \end{aligned}$$

Define  $\hat{a}$  as the constant term in the single-frequency model derived in C.1

$$\hat{a} = \frac{1-\gamma}{\beta} \left( \mu - \frac{1}{2} \gamma \sigma^2 \right) + \frac{1}{\beta} b_\lambda \kappa_\lambda \bar{\lambda}.$$

Then

$$\begin{aligned} \lim_{\sigma_\lambda \rightarrow 0} (\hat{a} + b_\lambda \lambda_t) &= \lim_{\sigma_\lambda \rightarrow 0} (\hat{a} + b_\lambda \bar{\lambda}) \\ &= \frac{1-\gamma}{\beta} \left( \mu - \frac{1}{2} \gamma \sigma^2 \right) + (\kappa_\lambda + \beta) \frac{\bar{\lambda}}{\beta} \lim_{\sigma_\lambda \rightarrow 0} b_\lambda \\ &= \frac{1-\gamma}{\beta} \left( \mu - \frac{1}{2} \gamma \sigma^2 \right) + \frac{E_\nu [e^{(1-\gamma)Z} - 1] \bar{\lambda}}{\beta}, \end{aligned}$$

where we assume that  $\lambda_0 = \bar{\lambda}$  and therefore that  $\lambda_t = \bar{\lambda}$  for all  $t$ .

Finally,

$$\begin{aligned} \lim_{\sigma_\lambda \rightarrow 0} \frac{\pi_t}{\pi_0} &= \exp \left\{ \left( -\beta - \beta \lim_{\sigma_\lambda \rightarrow 0} (\hat{a} + b_\lambda \bar{\lambda}) \right) t \right\} \left( \frac{C_t}{C_0} \right)^{-\gamma} \\ &\quad \exp \left\{ \left( -\beta - (1-\gamma) \left( \mu - \frac{1}{2} \gamma \sigma^2 \right) - E_\nu [e^{(1-\gamma)Z} - 1] \bar{\lambda} \right) t \right\} \left( \frac{C_t}{C_0} \right)^{-\gamma}, \end{aligned}$$

which is equivalent to the result one obtains by calculating the state price density in the iid case. As above, this result requires that we choose the lower of the two roots.

### C.3 An isomorphism with power preferences under the iid assumption

In this section we show that, in an iid model, ratios of the state price density at different times implied by power utility are the same as those implied by recursive utility assuming the discount rate is adjusted appropriately. Thus the power utility model and the recursive utility model are isomorphic when the endowment process is iid.

Let  $\pi_{p,t}$  be the state price density assuming power utility with discount rate  $\beta_p$  and relative risk aversion  $\gamma$ . Then

$$\frac{\pi_{p,t}}{\pi_{p,0}} = e^{-\beta_p t} \left( \frac{C_t}{C_0} \right)^{-\gamma}.$$

For convenience, let  $\pi_t$  be the state price density for recursive utility (with EIS equal to one). As shown in Appendix C.2,

$$\frac{\pi_t}{\pi_0} = e^{((1-\gamma)(-\mu + \frac{1}{2}\gamma\sigma^2) - \bar{\lambda}E_\nu[e^{(1-\gamma)Z} - 1] - \beta)t} \left( \frac{C_t}{C_0} \right)^{-\gamma}.$$

It follows that, for  $\beta$  given by

$$\beta = \beta_p + (1 - \gamma) \left( -\mu + \frac{1}{2}\gamma\sigma^2 \right) - \bar{\lambda}E_\nu [e^{(1-\gamma)Z} - 1],$$

ratios of the state price densities are the same.

## D Transform analysis

The normalized put option price is given as

$$P^n(\lambda_t, \xi_t, T - t; K^n) = E_t \left[ \frac{\pi_T}{\pi_t} \left( K^n - \frac{F_T}{F_t} \right)^+ \right]. \quad (\text{D.1})$$

It follows from (14), (15), and (B.21) that

$$\begin{aligned} \frac{\pi_T}{\pi_t} &= \exp \left\{ \int_t^T -\beta(1 + a + b_\lambda \lambda_s + b_\xi \xi_s) ds - \gamma \log \left( \frac{C_T}{C_t} \right) + b_\lambda(\lambda_T - \lambda_t) + b_\xi(\xi_T - \xi_t) \right\} \\ \frac{F_T}{F_t} &= \exp \left\{ \phi \log \left( \frac{C_T}{C_t} \right) + b_{\phi\lambda}^*(\lambda_T - \lambda_t) + b_{\phi\xi}^*(\xi_T - \xi_t) \right\}, \end{aligned}$$

where  $b_\lambda$ ,  $b_\xi$ ,  $b_{\phi\lambda}^*$  and  $b_{\phi\xi}^*$  are constants defined by (8), (9), (B.19), and (B.20), respectively.

To use the method of Duffie, Pan, and Singleton (2000), it is helpful to write down the following stochastic process, which, under our assumptions, is well-defined for given  $\lambda_t$  and  $\xi_t$ :

$$X_\tau = \begin{bmatrix} \log C_{t+\tau} - \log C_t \\ \lambda_{t+\tau} \\ \xi_{t+\tau} \end{bmatrix}.$$

Note that the  $\{X_\tau\}$  process is defined purely for mathematical convenience. We further define

$$d_1 = \begin{bmatrix} 0 \\ b_\lambda \\ b_\xi \end{bmatrix}, \quad d_2 = \begin{bmatrix} -\gamma \\ b_\lambda \\ b_\xi \end{bmatrix}, \quad d_3 = \begin{bmatrix} 0 \\ b_{\phi\lambda}^* \\ b_{\phi\xi}^* \end{bmatrix}, \quad d_4 = \begin{bmatrix} \phi \\ b_{\phi\lambda}^* \\ b_{\phi\xi}^* \end{bmatrix}.$$

Using this notation, (D.1) can be rewritten as

$$\begin{aligned}
P^n(\lambda_t, \xi_t, T - t; K^n) &= K^n E_t \left[ e^{-\int_0^{T-t} R(X_\tau) d\tau + d_2^\top X_{T-t} - d_1^\top X_0} \mathbf{1}_{\left\{\frac{F_T}{F_t} \leq K^n\right\}} \right] \\
&\quad - E_t \left[ e^{-\int_0^{T-t} R(X_\tau) d\tau + (d_2 + d_4)^\top X_{T-t} - (d_1 + d_3)^\top X_0} \mathbf{1}_{\left\{\frac{F_T}{F_t} \leq K^n\right\}} \right] \quad (\text{D.2})
\end{aligned}$$

where

$$\begin{aligned}
R(X_\tau) &= \beta d_1^\top X_\tau + \beta(1 + a) \\
\mathbf{1}_{\left\{\frac{F_T}{F_t} \leq K^n\right\}} &= \mathbf{1}_{\left\{d_4^\top X_{T-t} \leq \log K^n + d_3^\top X_0\right\}}.
\end{aligned}$$

Since  $\{X_\tau\}$  is an affine process in the sense defined by Duffie, Pan, and Singleton (2000), (D.2) characterizes the put option price in terms of expectations that can be computed using their transform analysis. Specifically, if we define

$$\mathcal{G}_{p,q}(y; X_0, T - t) \equiv E \left[ e^{-\int_0^{T-t} R(X_\tau) d\tau} e^{p^\top X_{T-t}} \mathbf{1}_{\{q^\top X_{T-t} \leq y\}} \right], \quad (\text{D.3})$$

then the normalized put price is expressed as

$$\begin{aligned}
P^n(\lambda_t, \xi_t, T - t; K^n) &= e^{-d_1^\top X_0} K^n \mathcal{G}_{d_2, d_4}(\log K^n + d_3^\top X_0; X_0, T - t) \\
&\quad - e^{-(d_1 + d_3)^\top X_0} K^n \mathcal{G}_{d_2 + d_4, d_4}(\log K^n + d_3^\top X_0; X_0, T - t),
\end{aligned}$$

where  $X_0 = [0, \lambda_t, \xi_t]$ . The terms written using the function  $\mathcal{G}$  can then be computed tractably using the transform analysis of Duffie et al: this analysis requires only the solution of a system of ordinary differential equations and a one-dimensional numerical integration.

## References

- Abel, Andrew, 1999, Risk premia and term premia in general equilibrium, *Journal of Monetary Economics* 43, 3–33.
- Andersen, Torben G., Nicola Fusari, and Viktor Todorov, 2013, The Risk Premia Embedded in Index Options, Working paper, Northwestern University.
- Backus, David, Mikhail Chernov, and Ian Martin, 2011, Disasters Implied by Equity Index Options, *The Journal of Finance* 66, 1969–2012.
- Bansal, Ravi, Dana Kiku, and Amir Yaron, 2012, An Empirical Evaluation of the Long-Run Risks Model for Asset Prices, *Critical Finance Review* 1, 183–221.
- Bansal, Ravi, and Amir Yaron, 2004, Risks for the long-run: A potential resolution of asset pricing puzzles, *Journal of Finance* 59, 1481–1509.
- Barro, Robert J., 2006, Rare disasters and asset markets in the twentieth century, *Quarterly Journal of Economics* 121, 823–866.
- Barro, Robert J., and Tao Jin, 2011, On the size distribution of macroeconomic disasters, *Econometrica* 79, 1567–1589.
- Barro, Robert J., and José F. Ursúa, 2008, Macroeconomic crises since 1870, *Brookings Papers on Economic Activity* no. 1, 255–350.
- Bates, David S., 2000, Post-'87 crash fears in the S&P 500 futures option market, *Journal of Econometrics* 94, 181–238.
- Bates, David S., 2008, The market for crash risk, *Journal of Economic Dynamics and Control* 32, 2291–2321.

- Benzoni, Luca, Pierre Collin-Dufresne, and Robert S. Goldstein, 2011, Explaining asset pricing puzzles associated with the 1987 market crash, *Journal of Financial Economics* 101, 552 – 573.
- Black, Fischer, and Myron Scholes, 1973, The Pricing of Options and Corporate Liabilities, *Journal of Political Economy* 81, 637–654.
- Bollerslev, Tim, and Viktor Todorov, 2011, Tails, Fears, and Risk Premia, *The Journal of Finance* 66, 2165–2211.
- Broadie, Mark, Mikhail Chernov, and Michael Johannes, 2007, Model specification and risk premia: Evidence from futures options, *Journal of Finance* 62, 1453–1490.
- Buraschi, Andrea, and Alexei Jiltsov, 2006, Model Uncertainty and Option Markets with Heterogeneous Beliefs, *The Journal of Finance* 61, 2841–2897.
- Campbell, John Y., 2003, Consumption-based asset pricing, in G. Constantinides, M. Harris, and R. Stulz, eds.: *Handbook of the Economics of Finance, vol. 1b* (Elsevier Science, North-Holland ).
- Campbell, John Y., 2008, Risk and return in stocks and bonds, Lecture 2, Princeton Lectures in Finance.
- Campbell, John Y., and John H. Cochrane, 1999, By force of habit: A consumption-based explanation of aggregate stock market behavior, *Journal of Political Economy* 107, 205–251.
- Campbell, John Y., and Robert J. Shiller, 1988, The dividend-price ratio and expectations of future dividends and discount factors, *Review of Financial Studies* 1, 195–228.

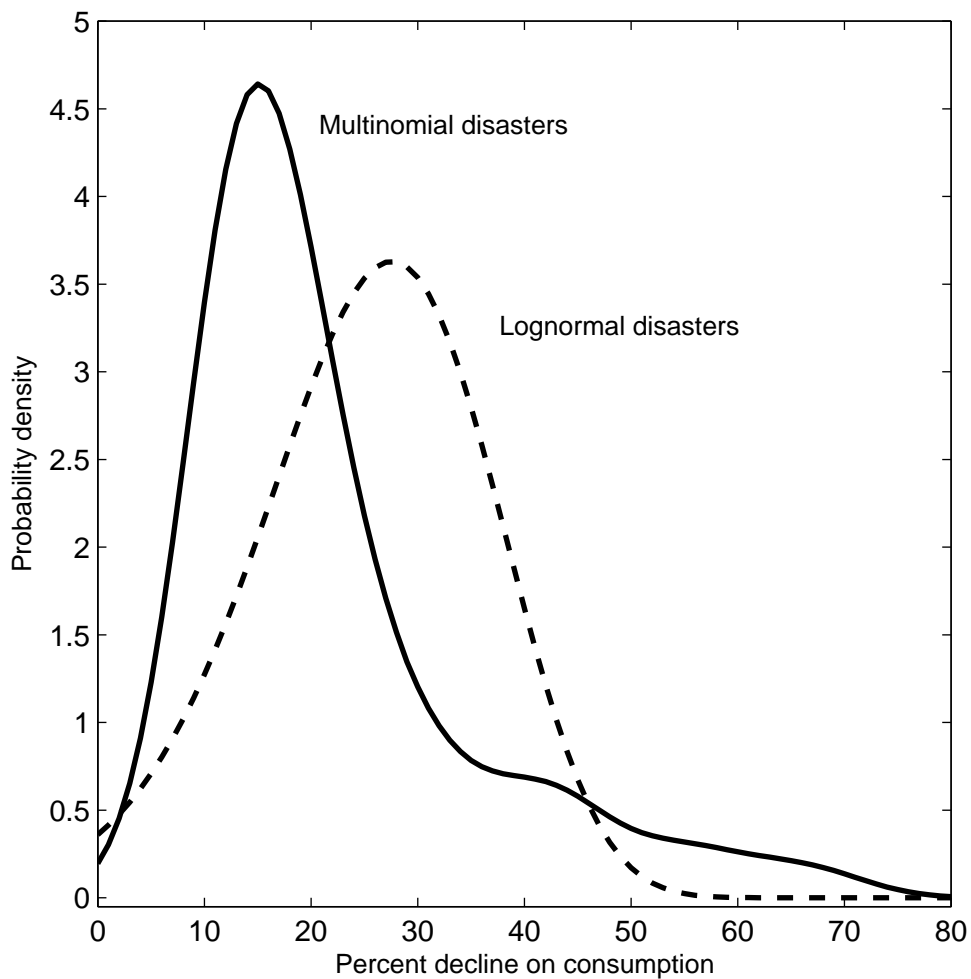
- Chacko, George, and Luis Viceira, 2005, Dynamic consumption and portfolio choice with stochastic volatility in incomplete markets, *Review of Financial Studies* 18, 1369–1402.
- Chen, Hui, Winston Wei Dou, and Leonid Kogan, 2013, Measuring the “Dark Matter” in Asset Pricing Models, Working paper, MIT.
- Christoffersen, Peter, Steven Heston, and Kris Jacobs, 2009, The Shape and Term Structure of the Index Option Smirk: Why Multifactor Stochastic Volatility Models Work So Well, *Management Science* 55, 1914–1932.
- Christoffersen, Peter, and Kris Jacobs, 2004, The importance of the loss function in option valuation, *Journal of Financial Economics* 72, 291–318.
- Coval, Joshua D., and Tyler Shumway, 2001, Expected option returns, *The Journal of Finance* 56, 983–1009.
- Cox, John C., Jonathan C. Ingersoll, and Stephen A. Ross, 1985, A theory of the term structure of interest rates, *Econometrica* 53, 385–408.
- Drechsler, Itamar, 2013, Uncertainty, Time-Varying Fear, and Asset Prices, *The Journal of Finance* 68, 1843–1889.
- Drechsler, Itamar, and Amir Yaron, 2011, What’s vol got to do with it, *Review of Financial Studies* 24, 1–45.
- Du, Du, 2011, General equilibrium pricing of options with habit formation and event risks, *Journal of Financial Economics* 99, 400–426.
- Duffie, Darrell, and Larry G Epstein, 1992, Asset pricing with stochastic differential utility, *Review of Financial Studies* 5, 411–436.

- Duffie, Darrell, Jun Pan, and Kenneth Singleton, 2000, Transform analysis and asset pricing for affine jump-diffusions, *Econometrica* 68, 1343–1376.
- Duffie, Darrell, and Costis Skiadas, 1994, Continuous-time asset pricing: A utility gradient approach, *Journal of Mathematical Economics* 23, 107–132.
- Dumas, Bernard, Jeff Fleming, and Robert E. Whaley, 1998, Implied Volatility Functions: Empirical Tests, *The Journal of Finance* 53, 2059–2106.
- Epstein, Larry, and Stan Zin, 1989, Substitution, risk aversion and the temporal behavior of consumption and asset returns: A theoretical framework, *Econometrica* 57, 937–969.
- Eraker, Bjørn, 2004, Do stock prices and volatility jump? Reconciling evidence from spot and option prices, *The Journal of Finance* 59, 1367–1404.
- French, Kenneth R., G. William Schwert, and Robert F. Stambaugh, 1987, Expected stock returns and volatility, *Journal of Financial Economics* 19, 3–29.
- Gabaix, Xavier, 2012, An exactly solved framework for ten puzzles in macro-finance, *Quarterly Journal of Economics* 127, 645–700.
- Gallant, A. Ronald, Chien-Te Hsu, and George Tauchen, 1999, Using Daily Range Data to Calibrate Volatility Diffusions and Extract the Forward Integrated Variance, *Review of Economics and Statistics* 81, 617–631.
- Gao, George P., and Zhaogang Song, 2013, Rare disaster concerns everywhere, Working paper, Cornell University.
- Gourio, François, 2012, Disaster risk and business cycles, *American Economic Review* 102, 2734–2766.

- Kelly, Bryan T., Lubos Pastor, and Pietro Veronesi, 2014, The Price of Political Uncertainty: Theory and Evidence from the Option Market, Working paper, University of Chicago.
- Liu, Jun, Jun Pan, and Tan Wang, 2005, An equilibrium model of rare-event premia and its implication for option smirks, *Review of Financial Studies* 18, 131–164.
- Longstaff, Francis A., and Monika Piazzesi, 2004, Corporate earnings and the equity premium, *Journal of Financial Economics* 74, 401–421.
- Neuberger, Anthony, 2012, Realized Skewness, *Review of Financial Studies* 25, 3423–3455.
- Nowotny, Michael, 2011, Disaster begets crisis: The role of contagion in financial markets, Working paper, Boston University.
- Pan, Jun, 2002, The jump-risk premia implicit in options: evidence from an integrated time-series study, *Journal of Financial Economics* 63, 3–50.
- Rietz, Thomas A., 1988, The equity risk premium: A solution, *Journal of Monetary Economics* 22, 117–131.
- Rubinstein, Mark, 1994, Implied Binomial Trees, *The Journal of Finance* 49, 771–818.
- Santa-Clara, Pedro, and Shu Yan, 2010, Crashes, Volatility, and the Equity Premium: Lessons from S&P 500 Options, *Review of Economics and Statistics* 92, 435–451.
- Shaliastovich, Ivan, 2009, Learning, Confidence and Option Prices, working paper, University of Pennsylvania.
- Shaliastovich, Ivan, 2015, Learning, confidence, and option prices, *Journal of Econometrics* 187, 18–42.

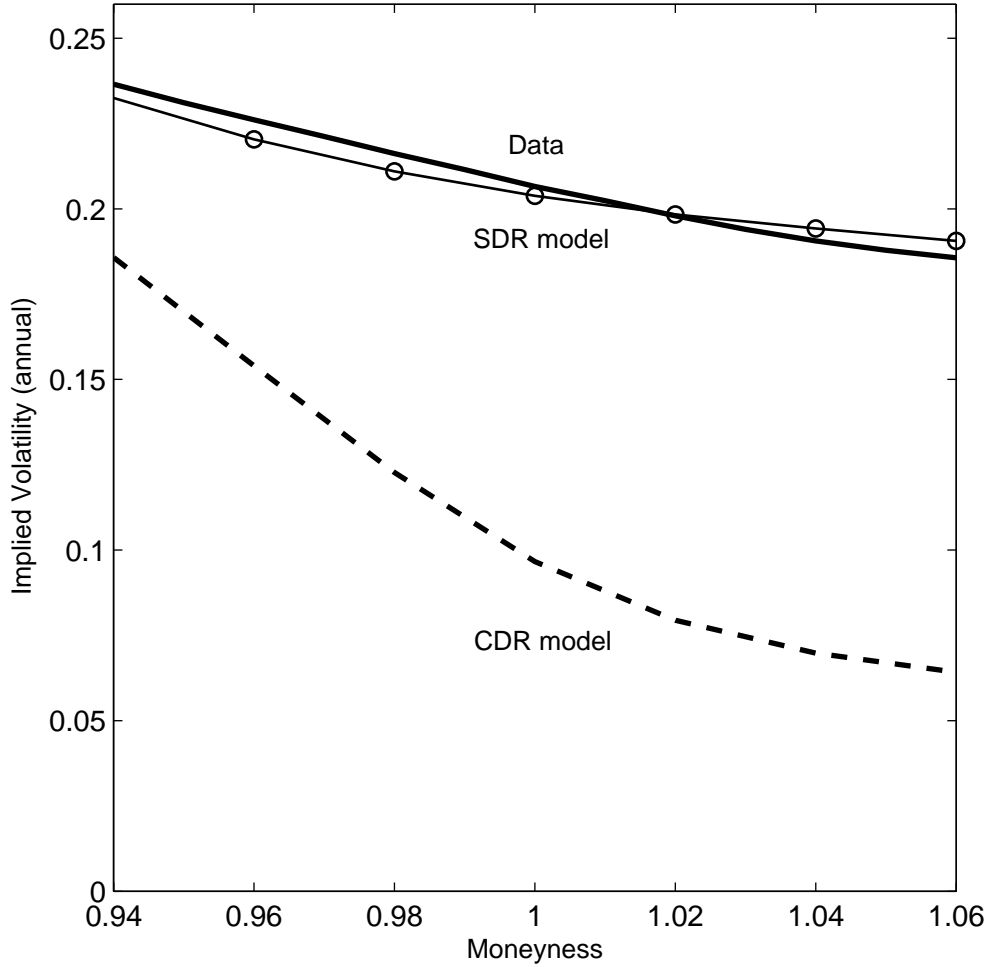
- Shiller, Robert J., 1981, Do stock prices move too much to be justified by subsequent changes in dividends?, *American Economic Review* 71, 421–436.
- Stutzer, Michael, 1996, A Simple Nonparametric Approach to Derivative Security Valuation, *The Journal of Finance* 51, 1633.
- Tallarini, Thomas D., 2000, Risk-sensitive real business cycles, *Journal of Monetary Economics* 45, 507–532.
- Tauchen, George, 2005, Stochastic volatility in general equilibrium, Working paper, Duke University.
- Wachter, Jessica A., 2013, Can time-varying risk of rare disasters explain aggregate stock market volatility?, *The Journal of Finance* 68, 987–1035.
- Weil, Philippe, 1990, Nonexpected utility in macroeconomics, *Quarterly Journal of Economics* 105, 29–42.
- Yan, Shu, 2011, Jump risk, stock returns, and slope of implied volatility smile, *Journal of Financial Economics* 99, 216–233.

Figure 1: Probability density functions for consumption declines



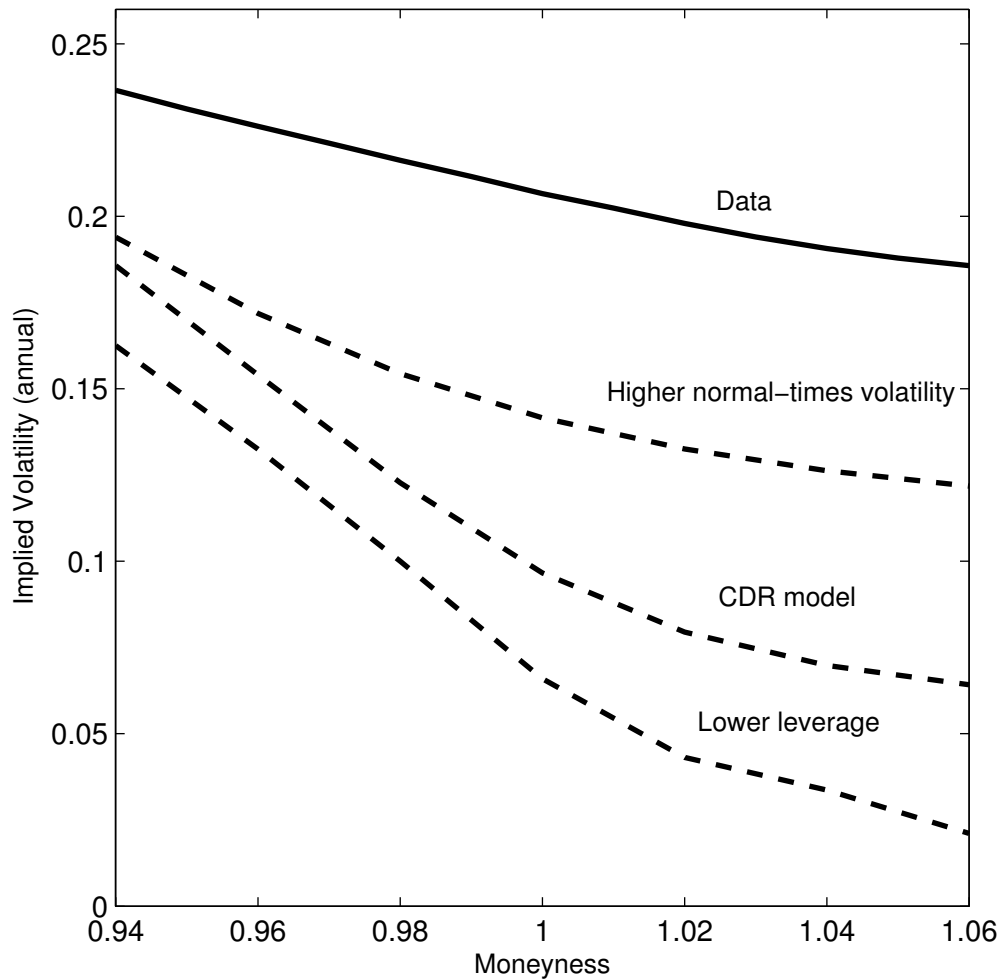
Notes: The probability density functions (pdfs) for consumption declines for log-normally distributed disasters and for the multinomial distribution assumed in the stochastic disaster risk (SDR) model. In the case of the SDR model, the pdf approximates the multinomial distribution from Barro and Ursúa (2008). The exact multinomial distribution is used to calculate the results in the paper. The pdfs are for the quantities  $1 - e^Z$  in each model.

Figure 2: Average implied volatilities in the SDR and CDR models



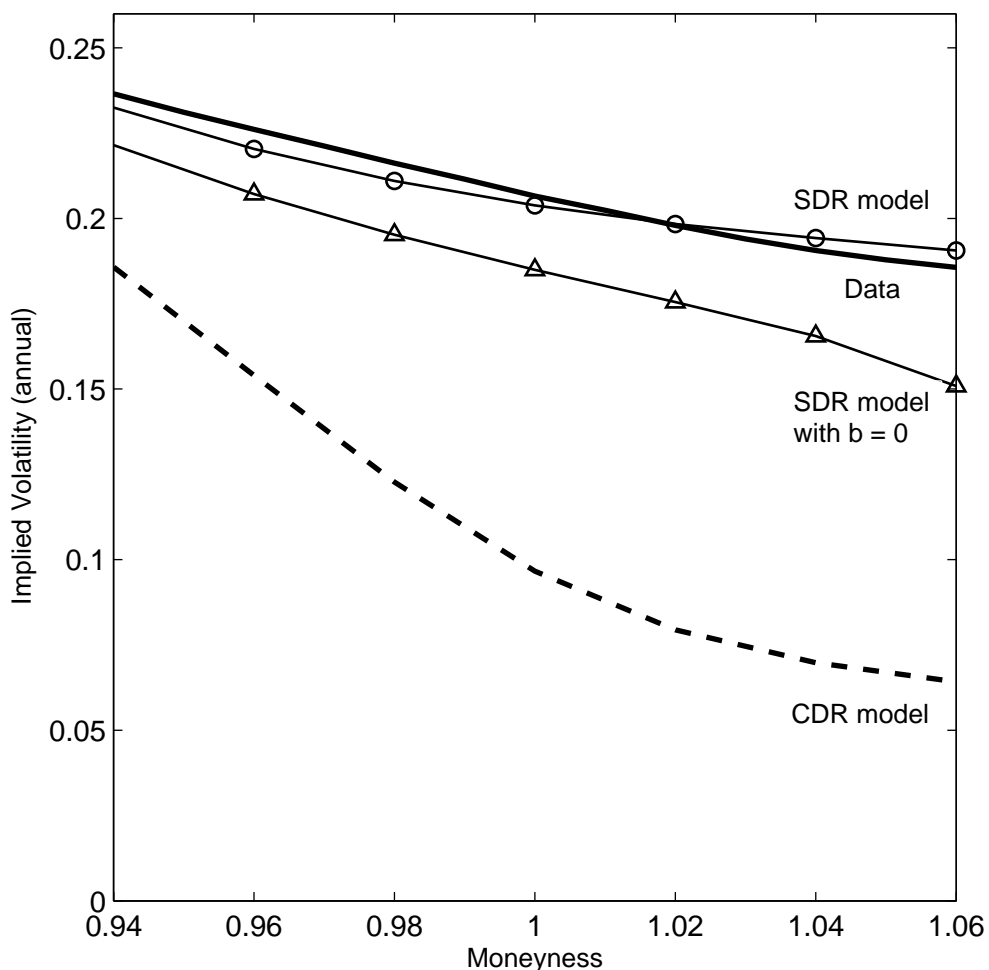
Notes: Average implied volatilities for 3-month options as a function of moneyness for the single-frequency stochastic disaster risk (SDR) model, for the constant disaster risk (CDR) model and in the data. Average implied volatilities are shown as functions of moneyness, defined as the exercise price divided by the asset price.

Figure 3: Comparative statics for the CDR model



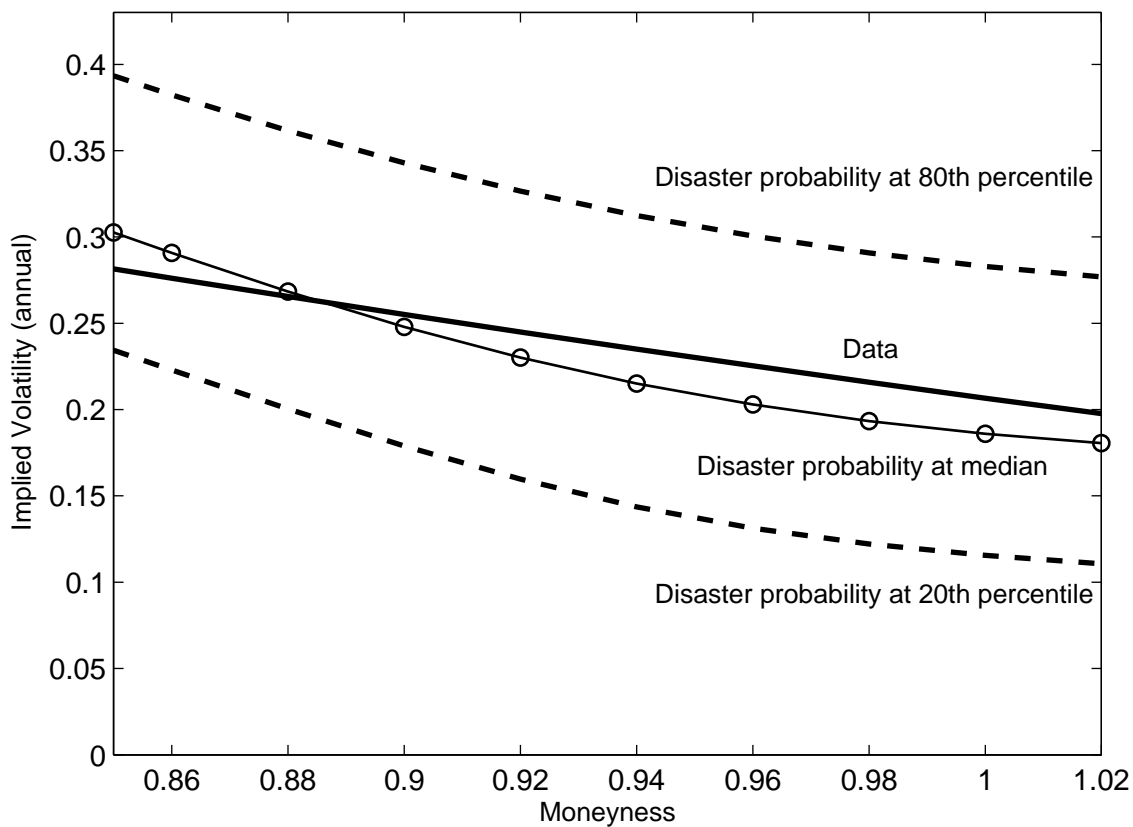
Notes: Implied volatilities for 3-month options as a function of moneyness in the data and for three parameterization of the constant disaster risk (CDR) model. The line labeled “CDR” shows the benchmark calibration. The line labeled “higher normal-times volatility” raises the volatility of consumption shocks that are not associated with disasters from 1% to 2% per annum but keeps all other parameters, including the consumption disaster distribution, the same. The line labeled “lower leverage” lowers the term multiplying dividends from 5.1 to 2.6, while keeping all other parameters the same.

Figure 4: The premium for volatility risk



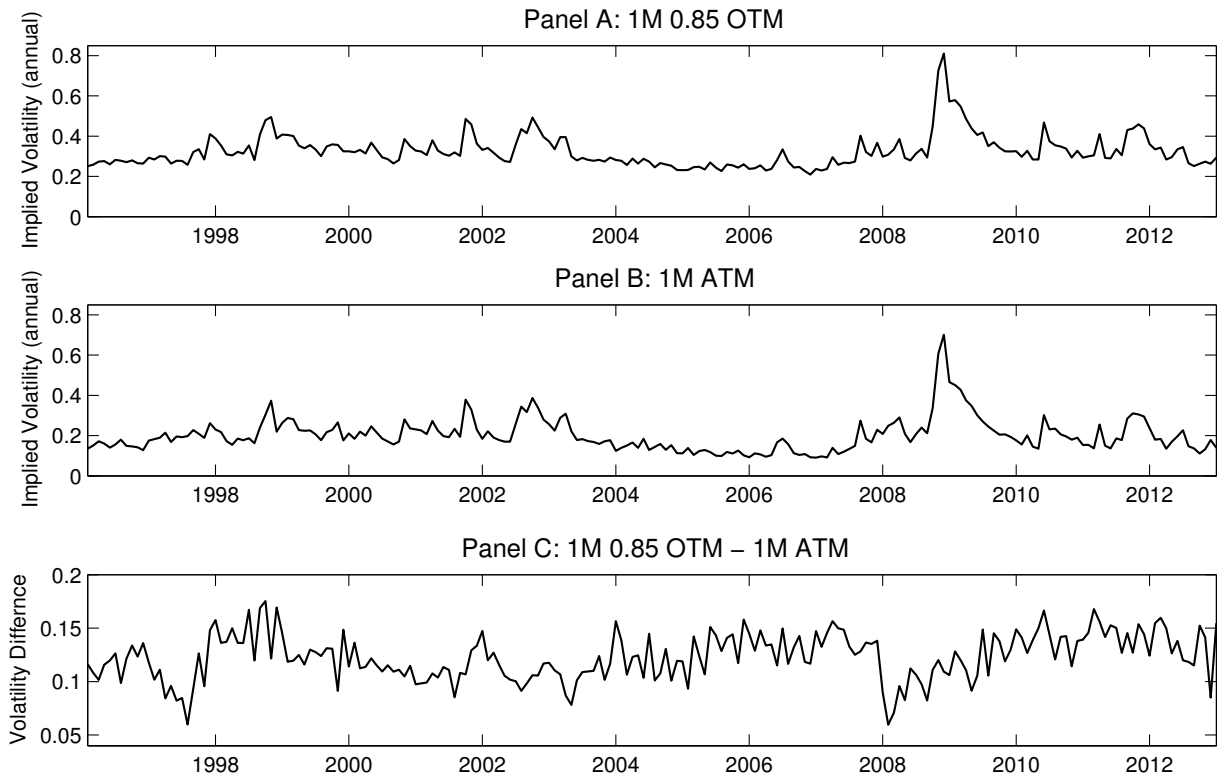
Notes: Implied volatilities for 3-month options as a function of moneyness in the data, in the CDR model, and in the (single-frequency) SDR model. Also shown are implied volatilities in the SDR model computed under the assumption that the premium associated with time-variation in the disaster probability is equal to zero (SDR model with  $b_\lambda = 0$ ). Note both the benchmark and the  $b_\lambda = 0$  version of the SDR model are dynamic models. The CDR model is iid.

Figure 5: Implied volatilities at the 20th, 50th, and 80th percentile disaster probability



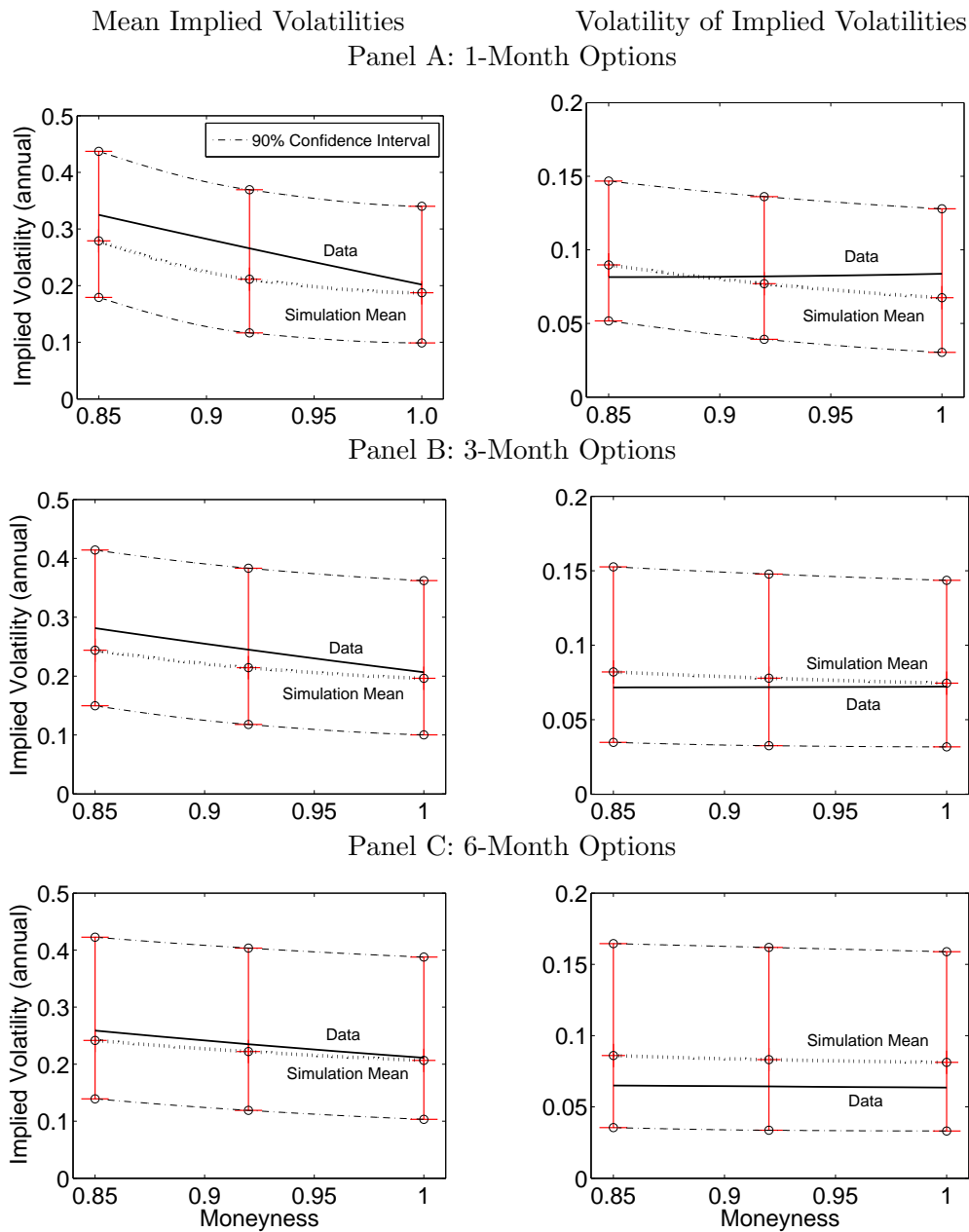
Notes: Implied volatilities on 3-month options in the single-frequency SDR model for the disaster probability at the 20th, 50th, and 80th percentile. Also shown are the average implied volatilities in the data.

Figure 6: 1-month implied volatility time series



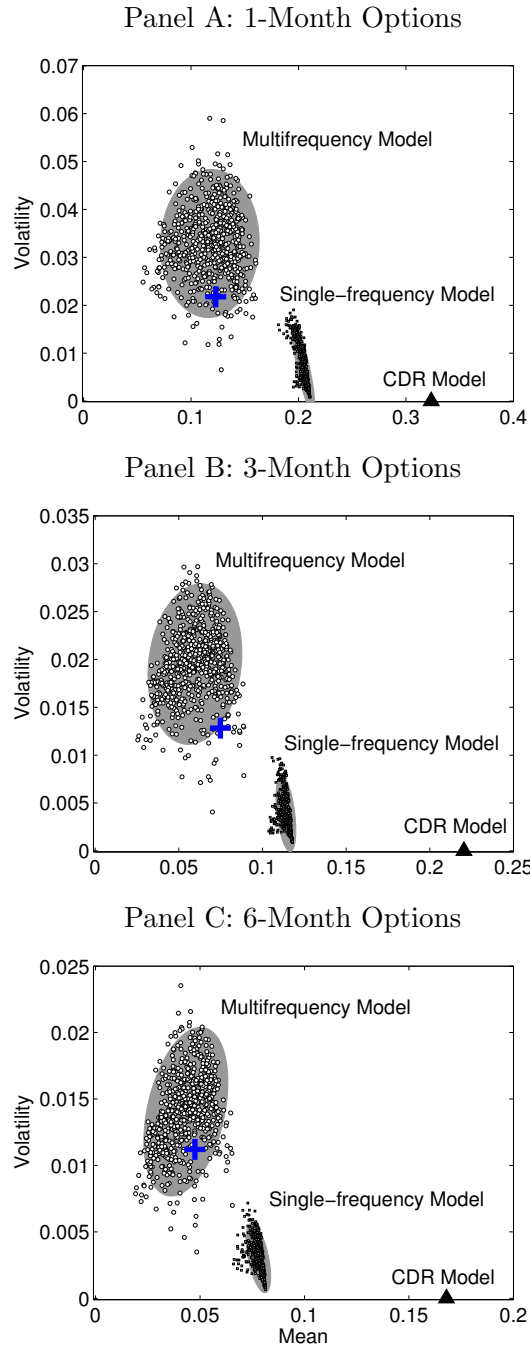
Notes: Monthly time series of implied volatilities on 1-month options in the data and of the difference in implied volatilities. Implied volatilities are calculated for ATM options and OTM options with moneyness equal to 0.85.

Figure 7: Means and standard deviations of implied volatilities in simulated data



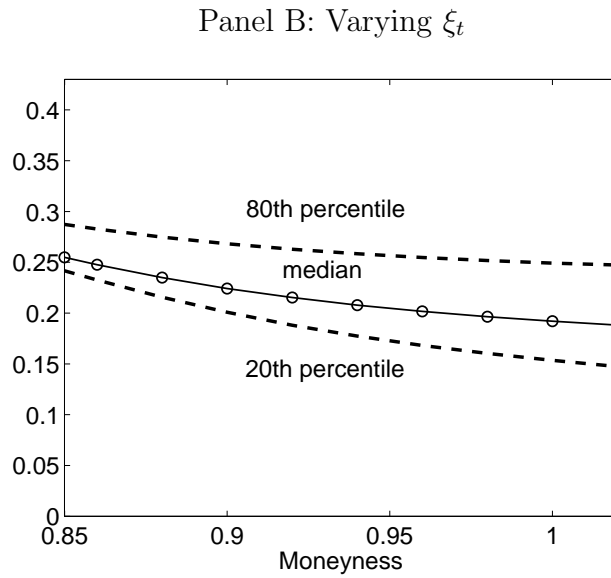
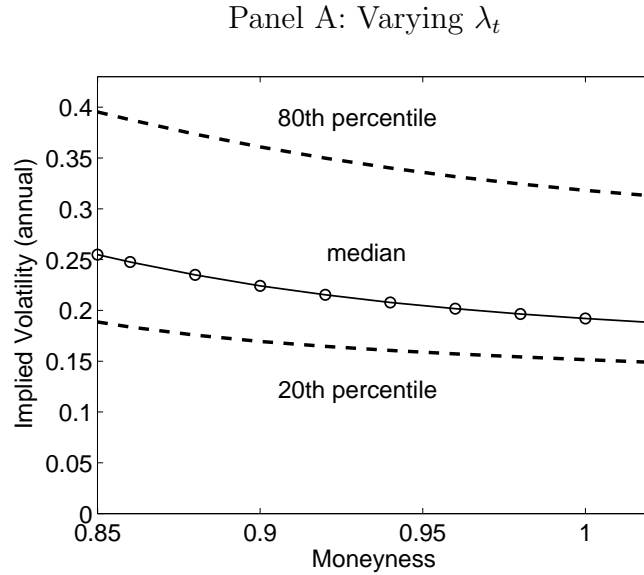
Notes: We simulate 1000 samples of length 17 years from the multifrequency SDR model. For each sample path, we compute the mean and volatility of implied volatilities at three different moneyness levels and for three maturities. The dotted line shows the means of these statistics across sample paths, while the dashed-dotted lines show 95th and 5th percentiles. The solid line shows the data.

Figure 8: Means and volatilities of the volatility skew



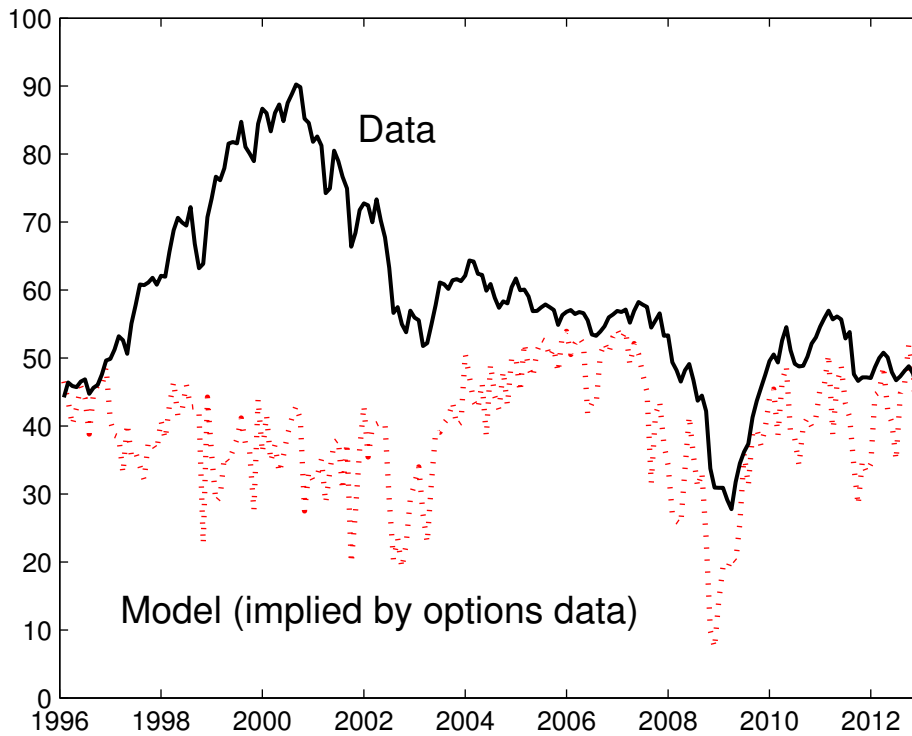
Notes: We simulate 1000 samples of length 17 years from the single- and multi-frequency SDR models. For each sample path, we compute the mean and volatility of the slope of the volatility skew, defined as the difference in implied volatilities between the 0.85 OTM and the ATM put options. We plot the volatilities and means of the implied volatility slope for each sample path for the multifrequency model (circles) and the single-frequency model (squares), as well as for the CDR model (triangle) and the data (cross). The shaded regions denote 95% confidence ellipses based on the models.

Figure 9: Implied volatilities as functions of the state in the multifrequency SDR model



Notes: Implied volatilities on 3-month options as functions of moneyness for the multifrequency SDR model. The figures show the effects of varying the state variables  $\lambda_t$  (the disaster probability) and  $\xi_t$  (the value to which  $\lambda_t$  reverts). Panel A sets  $\xi_t$  equal to its median value and varies  $\lambda_t$ , while Panel B sets  $\lambda_t$  equal to its median value and varies  $\xi_t$ .

Figure 10: The price-dividend ratio in the data and in the model



Notes: The solid line shows the time series of the price-dividend ratio on the data. The red line shows the price-dividend ratio implied by the multifrequency SDR model for state prices chosen to fit the one-month ATM and OTM (0.85 moneyness) put options.

Table 1: Parameter values

	SDR	CDR
Relative risk aversion $\gamma$	3.0	5.19
EIS $\psi$	1	1
Rate of time preference $\beta$	0.0120	0.0189
Average growth in consumption (normal times) $\mu$	0.0252	0.0231
Volatility of consumption growth (normal times) $\sigma$	0.020	0.010
Leverage $\phi$	2.6	5.1429
Average probability of a rare disaster $\bar{\lambda}$	0.0355	0.010
Mean reversion $\kappa$	0.080	NA
Volatility parameter $\sigma_\lambda$	0.067	0

Notes: Parameters for the single-frequency stochastic disaster risk (SDR) model and for the benchmark constant disaster risk (CDR) model, in annual terms.

Table 2: Parameter values for the multifrequency SDR model

Panel A: $\lambda$ process	
Mean reversion $\kappa_\lambda$	0.2
Volatility parameter $\sigma_\lambda$	0.1576
Panel B: $\xi$ process	
Mean $\xi$	0.02
Mean reversion $\kappa_\xi$	0.1
Volatility parameter $\sigma_\xi$	0.0606
Panel C: Population statistics of $\lambda$	
Median	0.0037
Standard deviation	0.0386
AR(1) coefficient	0.9858

Notes: Parameter values for the multifrequency SDR model. The processes are as follows:

$$\begin{aligned}
 d\lambda_t &= \kappa_\lambda(\xi_t - \lambda_t)dt + \sigma_\lambda\sqrt{\lambda_t}dB_{\lambda,t} \\
 d\xi_t &= \kappa_\xi(\bar{\xi} - \xi_t)dt + \sigma_\xi\sqrt{\xi_t}dB_{\xi,t}.
 \end{aligned}$$

Panels A and B show parameter values expressed in annual terms. Panel C shows population statistics for the disaster probability  $\lambda_t$  calculated by simulation at a monthly frequency (while the median disaster probability is annual, the AR(1) coefficient should be interpreted as monthly).

Table 3: Moments for the government bill rate and the market return for the multifrequency SDR model

	Data	No-Disaster Simulations			All Simulations			Population
		0.05	0.50	0.95	0.05	0.50	0.95	
$E[R^b]$	1.25	1.68	2.96	3.46	-0.47	2.41	3.37	2.02
$\sigma(R^b)$	2.75	0.34	1.07	2.71	0.48	2.06	7.14	3.69
$E[R^m - R^b]$	7.25	5.40	8.01	12.36	5.30	8.49	14.25	9.00
$\sigma(R^m)$	17.8	13.24	19.26	27.91	14.59	22.59	34.38	24.13
Sharpe Ratio	0.41	0.32	0.42	0.55	0.26	0.39	0.53	0.37
$\exp(E[p - d])$	32.5	28.96	40.63	48.88	22.93	36.95	47.41	35.36
$\sigma(p - d)$	0.43	0.15	0.27	0.47	0.17	0.33	0.59	0.43
$AR1(p - d)$	0.92	0.59	0.79	0.91	0.62	0.82	0.92	0.90

Notes: Data moments are calculated using annual data from 1947 to 2010. Population moments are calculated from simulating data from the multifrequency stochastic disaster risk (SDR) model at a monthly frequency for 600,000 years and then aggregating monthly growth rates to an annual frequency. We also simulate 100,000 60-year samples and report the 5th, 50th and 95th percentile for each statistic, both from the full set of simulations and for the subset of samples for which no disasters occur.  $R^b$  denotes the government bill return,  $R^m$  denotes the return on the aggregate market and  $p - d$  denotes the log price-dividend ratio.